JOURNAL OF GEOPHYSICAL RESEARCH, VOL. 101, NO. B5, PAGES 11,729–11,746, MAY 10, 1996

Geochemical stratigraphy of lava flows sampled by the Hawaii Scientific Drilling Project

J. M. Rhodes

Department of Geosciences, University of Massachusetts, Amherst

Abstract. Geochemical discriminants are used to place the boundary between Mauna Loa flows and underlying Mauna Kea flows at a depth of about 280 m. At a given MgO content the Mauna Kea flows are lower in SiO_2 and total iron and higher in total alkali, TiO_2, and incompatible elements than the Mauna Loa lavas. The uppermost Mauna Kea lavas (280 to 340 m) contain alkali basalts interlayered with tholeiites and correlate with the postshield Hamakua Volcanics. In addition to total alkalis, the alkali basalts have higher TiO_2, P_2O_5, Sr, Ba, Ce, La, Zr, Nb, Y, and V relative to the tholeiites and lower Zr/Nb and Sr/Nb ratios. Some of the alkali basalts are extensively differentiated. Below 340 m all the flows are tholeiitic, with compositions broadly similar to the few "fresh" subaerial shield-building Mauna Kea tholeiites studied to date. High-MgO lavas are unusually abundant, although there is a wide range (7-28%) in MgO content reflecting olivine control. FeO/MgO relationships are used to infer parental picritic magmas with about 15 wt % MgO. Lavas with more MgO than this have accumulated olivine. The Mauna Loa lavas have compositional trends that are controlled by olivine crystallization and accumulation. They compare closely with trends for historical (1843-1984) flows, tending toward the depleted end of the spectrum. They are, though, much more MgO-rich (9-30%) than is typical for most historical and young (<30 ka) prehistoric lavas. The unusual abundance of high-MgO and picritic lavas is attributed to the likelihood that only large-volume, hot, mobile flows will reach Hilo Bay from the northeast rift zone. FeO/MgO relationships are used to infer parental picritic magmas with about 17 wt % MgO. Again, lavas with more MgO than this have accumulated olivine. Systematic changes in incompatible element ratios are used to argue that the magma supply rate has diminished over time. On the other hand, the relatively constant Zr/Nb and Sr/Nb ratios that compare closely with historical and young (<30 kyr) prehistoric flows are used to argue that the source components for these lavas in the Hawaiian plume have remained relatively uniform over the last 100 kyr.

Introduction

This paper reports major and trace element whole rock analyses of 94 selected individual flow units sampled throughout the core recovered by the Hawaii Scientific Drilling Project (HSDP). A subsequent, more comprehensive, study will examine every identified flow unit. Details of the drilling, and a summary and overview of the project are given by *Thomas et al.* [this issue] and *Stolper et al.* [this issue]. The primary goals of this preliminary study are: (1) to use geochemical data to identify flow units originating from Mauna Loa and Mauna Kea volcanoes, the depth to the boundary between them, and the extent to which the flows from these two volcanoes are interfingered; (2) to evaluate compositional variation with depth (increasing age), in particular the extent and distribution of tholeiitic, alkalic and transitional lavas, and whether there are systematic changes in composition over time; (3) to integrate the data on the Mauna Loa lavas from the drill hole with what is known about magmatic processes and the temporal evolution of Mauna Loa from extensive data on historical and prehistoric flows. *Yang et al.* [this issue] examine the Mauna Kea flow units in the drill hole from a similar perspective. As has been suggested by *Frey and Rhodes* [1993], it is from a detailed examination of temporal changes in lavas from the shield-building stage of Hawaiian volcanoes that we are likely to learn most about the dynamics of mantle plumes and associated magma production and volcanism.

Paper number 95JB03704.
0148-0227/96/95JB-03704$09.00

Analytical Methods

Because the drill site was located close to the coast and almost all of the core came from below sea level (*Thomas et al.*, this issue), extensive precautions were taken to minimize seawater contamination. About 300-600 g of core was coarse-crushed by hand in a high-carbon steel percussion mortar. This material was then flushed continuously in tap water for 1-2 days until the conductivity of the water was about 50-70 μS. Rinsing in deionized water in an ultrasonic bath followed further reducing the conductivity of the water to 2-3 μS. The coarse-crushed material was then dried in air and split into archival and analytical halves. About 150 g of the analytical portion was further crushed to about 100-200 mesh in a Spex tungsten carbide shatterbox. Aliquants of this powder were taken for X-ray fluorescence analysis (XRF). The major elements were measured on a fused La-bearing lithium borate glass disc using modifications of the methods of *Norrish and Hutton* [1969], the principle difference being that the sample was first ignited at 1000^{0}C for several hours in order to oxidize the iron to Fe^{3+} and to remove volatiles. All elements (including Na_2O) were measured simultaneously using a Siemens MRS-400 spectrometer. The trace elements Rb, Sr, Ba, La, Ce, Nb, Zr, Y, Pb, Zn, Ga, Ni, Cr, V were measured on pressed powder pellets using a Siemens SRS-1 sequential spectrometer. Intensities were corrected for nonlinear background, interelement interferences, and variations in mass

absorption coefficients, using methods modified from those of Norrish and Chappell [1967]. Mass absorption coefficients for elements with shorter characteristic wavelengths than the Fe-absorption edge were estimated from the intensity of the Compton radiation of the appropriate X-ray tube (Mo or Au) [*Reynolds*, 1967]. Mass absorption coefficients of elements with longer characteristic radiation than the Fe absorption edge were calculated from the Compton-derived mass absorption coefficients, after allowance was made for Fe and Ti intensities [*Walker*, 1973].

All samples were analyzed in duplicate, and averages of these analyses are reported in Table 1. Estimates of the accuracy and precision can be obtained from *Rhodes* [1988], and from data for the U.S.Geological Survey basalt standard BHVO-1 and multiple analyses of KIL-1919, an HSDP standard, which were analyzed concurrently with the HSDP samples (Table 2). KIL-1919 was collected by H. West from the same 1919 Kilauea flow as the U.S. geological Survey Hawaiian basalt standard BHVO-1. This flow is, however, slightly heterogeneous [*J. M.Rhodes*, unpublished data, 1995] and there are differences in composition between BHVO-1 and KIL-1919 (Table 2).

Discrimination

It has long been recognized that lavas from adjacent Hawaiian shield volcanoes often have distinctive compositions. These differences are clearest for the isotopic ratios of Sr and Pb [e.g., *O'Nions et al.*, 1977; *Tatsumoto*, 1978; *Frey and Rhodes*, 1993] but also extend to major elements [e.g., *Powers*, 1955; *Wright*, 1971; *Rhodes et al.*, 1989] and to the trace elements [e.g., *Budahn and Schmitt*, 1985; *Tilling et al.*, 1987; *Rhodes et al.*, 1989; *Frey and Rhodes*, 1993]. Several studies suggest that these differences may persist for many thousands of years and possibly longer than 100 kyrs [*Lipman et al.*,1990; *Frey and Rhodes*, 1993; *Chen et al.*, 1996]. Some Hawaiian shields, however, such as that of Kahoolawe [*West et al.*, 1987], exhibit considerable variation. *Frey and Rhodes* [1993] propose that the best discriminants between adjacent shields are TiO_2 among the major elements and Nb among the trace elements. Several recent studies of Hawaiian shield volcanoes [e.g. *Frey and Rhodes*, 1993; *Frey et al.*, 1994; *Roden et al.*, 1994; *Rhodes and Hart*, 1995; *Kurz et al.*, 1995; *Chen et al.*, 1996] show that ratios involving Nb correlate with Sr and Pb isotopes and that there is no such coherence between these isotopic ratios and other incompatible element ratios. Presumably, the isotopic ratios, and those ratios involving Nb, are reflecting different proportions of source components in the Hawaiian plume, whereas the other incompatible element ratios are more sensitive to the melting history. Consequently, ratios involving these elements (e.g., TiO_2/Al_2O_3, Ti/Y, Zr/Nb, Sr/Nb, Nb/Y) tend to be more useful discriminants than La/Yb, K/Y, Sr/Y, Zr/Y, etc.

Figure 1 compares data for historical Mauna Loa lavas [*Rhodes and Hart*, 1995] with subaerial Hamakua Volcanics and submarine lavas from the Mauna Kea shield [*Frey et al.*, 1990, 1991; *Yang and Frey*, 1994]. Although there is some slight overlap between Mauna Loa and Mauna Kea lavas, especially in the submarine Mauna Kea lavas, Figure 1 shows that Sr/Nb of about 28, Zr/Nb of about 12.5, and TiO_2/Al_2O_3 of about 0.17 provide useful discriminants between the Mauna Loa and Mauna Kea lavas. In combination, these discriminants are very effective. The range is much more extensive for Mauna Kea lavas than for the Mauna Loa lavas. In part, this is a consequence of the restricted age range of the Mauna Loa samples (141 years), but mostly it reflects the different ratios for tholeiitic and alkalic Mauna Kea lavas. The alkalic lavas tend to have lower Sr/Nb and Zr/Nb and higher TiO_2/Al_2O_3 than the tholeiitic lavas. Extreme values are found in the iron-enriched samples (Figure 1).

Figure 2 shows that these discriminants separate the HSDP data into three broad groups. One, with overall characteristics that are similar to the historical Mauna Loa lavas, comprises the uppermost flows sampled by the drill hole. The other two have the characteristics of Mauna Kea tholeiitic and alkalic lavas and are stratigraphically lower in the drill hole. Within these lower flows, the discriminants also effectively separate alkalic and tholeiitic lavas. The boundary between the Mauna Loa and Mauna Kea flows is therefore inferred to occur at a depth of about 280 m (Figure 3). Figure 3 also shows that the boundary between the flows from the two volcanoes is very sharp and that there is no clear evidence for interfingering throughout the drill hole.

Mauna Loa Lavas

All 280 m of the Mauna Loa lavas are tholeiitic (Figures 4 and 5). Compared with the underlying Mauna Kea tholeiitic lavas, they have slightly less total alkalis at a given SiO_2 content. This difference is primarily a function of the K_2O content, since Na_2O is essentially constant in tholeiitic lavas from both volcanoes at a fixed MgO content (Figures 6e and 6f). The lower K_2O content is probably a characteristic of these lavas (see below), but it may be caused in part by alteration and leaching of potassium. Several workers [e.g., *Lipman et al.*, 1990; *Frey et al.*, 1990, 1994] have shown that, particularly in regions of high tropical rainfall, the potassium and rubidium contents of Hawaiian lavas can be substantially reduced through low-temperature weathering. The K_2O/P_2O_5 of these altered lavas is typically less than 1.4, and often below 1.0. Fresh, historical Mauna Loa lavas have K_2O/P_2O_5 of about 1.6. Very few of the Mauna Loa drill hole lavas have values that are this high, and about a third of them have values less than 1.0, implying that they have probably lost some potassium and rubidium, and possibly even barium. Figure 6f shows very clearly that when compared with the regression line for historical Mauna Loa lavas, most of the samples contain much less K_2O. This is not the case for incompatible elements that are not as susceptible to alteration, such as TiO_2, Nb, Zr, (Figures 6, 7).

The Mauna Loa lavas have abundances of Al_2O_3, CaO, Na_2O, Ga, Ni, Cr, and V at a given MgO content similar to those of the underlying tholeiitic Mauna Kea lavas (Figures 6 and 7 and Table 1). SiO_2 tends to be slightly higher in the Mauna Loa samples, but there is considerable overlap. Conversely, FeO is slightly lower in Mauna Loa tholeiites than in those from Mauna Kea, and the MgO-FeO trends are different, but again there is some overlap (Figure 8). Incompatible element abundances (e.g., TiO_2, K_2O, P_2O_5, Rb, Sr, Ba, Ce, La, Zr, Nb), however, are consistently lower in the Mauna Loa samples (Figures 6 and 7 and Table 1). Y is an exception (Figure 7d): although it is slightly lower in the Mauna Loa lavas than in the Mauna Kea lavas, there is some overlap. These figures also show that the HSDP Mauna Loa flows have compositional trends that are very similar to those of historical lavas when compared with best fit regression lines for the historical data. There are three interesting exceptions, SiO_2, CaO, and Y. SiO_2 tends to be slightly lower in the HSDP samples at a given MgO content than in the historical lavas, whereas both CaO and Y are slightly higher. Sr and Nb also tend to be slightly lower in abundance when compared with the regression lines for historical lavas. They compare closely, however, with more depleted historical lavas erupted between 1880 and 1887 [*Rhodes and Hart*, 1995].

The Mauna Loa data form well-defined linear arrays that reflect olivine control. This is clearly illustrated by Figure 9, a plot of Al/(Mg+Fe) versus Mg/(Mg+Fe). An advantage of this kind of diagram is that the intersection of the olivine-control trend with the abscissa provides an estimate of the olivine composition dominating the trend [*Irvine*, 1979]. The regression line for the Mauna Loa data intersects an olivine composition along the abscissa of about $Fo_{89.5}$. This compares very closely with an olivine composition ($Fo_{89.7}$) derived from the regression of FeO with MgO (Figure 8). Melts in equilibrium with olivine of this composition will have an FeO/MgO of

Table 1. Chemical Composition of Lavas Sampled by the Hawaii Scientific Drilling Project

	Sample															
	R055-0.75	R068-1.25	R075-1.70	R083-3.70	R091-2.30	R096-1.80	R103-2.65	R108-4.45	R110-3.10	R111-0.90	R114-3.50	R117-0.80	R121-2.45	R126-0.90	R128-0.45	R129-5.50
Flow unit	11	13	14	15	15	16	17	19	20	21	23	27	28	29	30	32
Depth (m)	74.0	94.1	104.8	117.6	129.2	136.7	147.7	156.0	164.0	164.0	176.1	184.4	191.8	199.8	205.7	210.8
SiO_2	50.18	44.51	50.04	48.43	47.09	47.48	47.55	49.91	50.19	49.59	49.45	50.47	48.76	48.97	45.33	46.47
TiO_2	1.82	0.77	1.82	1.47	1.44	1.60	1.57	2.00	1.85	2.09	1.69	1.95	1.83	1.78	1.06	1.36
Al_2O_3	11.94	5.54	11.93	9.87	9.28	9.55	9.63	13.06	12.37	13.53	11.77	15.71	11.04	10.80	7.55	9.17
$Fe_2O_3^*$	12.05	12.44	11.90	12.00	12.61	12.72	12.77	12.74	12.51	12.71	12.92	11.03	12.25	12.23	12.29	12.17
MnO	0.17	0.17	0.17	0.17	0.18	0.18	0.17	0.18	0.18	0.18	0.18	0.16	0.17	0.17	0.17	0.17
MgO	12.16	29.77	11.90	17.40	19.73	18.59	18.67	9.54	10.75	9.03	12.30	6.89	14.65	15.09	26.12	21.55
CaO	9.23	5.01	9.70	8.43	7.44	7.60	7.65	10.13	9.64	10.28	9.18	10.97	8.84	8.65	5.70	7.08
Na_2O	2.13	1.05	2.26	1.76	1.59	1.70	1.69	2.26	2.23	2.19	1.97	2.55	1.98	1.83	1.29	1.61
K_2O	0.34	0.13	0.33	0.26	0.19	0.22	0.21	0.18	0.28	0.15	0.25	0.18	0.23	0.25	0.10	0.09
P_2O_5	0.20	0.09	0.21	0.17	0.14	0.16	0.15	0.20	0.18	0.20	0.16	0.19	0.17	0.17	0.10	0.14
Total	100.21	99.48	100.25	99.96	99.70	99.80	100.06	100.20	100.18	99.95	99.88	100.09	99.92	99.94	99.71	99.81
Mg#	0.690	0.840	0.688	0.761	0.775	0.763	0.763	0.622	0.654	0.610	0.677	0.579	0.725	0.731	0.824	0.796
Rb	5.1	2.2	4.9	3.7	2.3	3.3	2.9	2.4	4.3	0.9	3.9	2.1	3.3	3.0	1.6	0.8
Sr	266	129	285	231	203	217	213	281	262	277	241	286	243	239	155	193
Ba	60	38	70	69	58	85	66	74	73	63	74	61	65	60	42	31
La	6	6	4	6	6	7	5	9	9	5	7	4	6	2	0	2
Ce	24	11	23	18	12	21	20	25	19	18	17	17	17	20	14	19
Nb	7.9	3.9	7.9	7.0	6.5	7.4	6.8	7.9	7.2	8.5	6.8	8.0	8.0	7.9	4.4	6.4
Zr	114	54	119	96	91	104	96	118	107	127	100	114	110	107	66	86
Y	20.8	9.8	21.9	18.1	16.0	19.1	16.9	23.8	21.1	24.5	20.3	24.4	20.3	20.0	14.5	18.4
Pb	4	1	2	3	3	3	2	3	2	2	4	1	2	2	3	4
Zn	100	99	105	97	105	102	109	96	97	113	103	87	110	106	106	108
Ga	17	10	18	15	15	15	16	21	18	20	17	21	16	17	11	14
Ni	415	1277	330	581	782	707	753	152	208	147	283	111	543	580	1440	1114
Cr	611	2165	880	1272	1271	1145	1131	387	524	473	697	229	882	898	1257	976
V	231	133	215	185	196	205	199	210	199	269	220	247	225	218	150	194

Table 1. (continued)

	Sample															
	R133-6.10	R135-3.50	R142-1.60	R150-0.05	R153-3.05	R158-0.05	R159-4.10	R160-5.75	R164-1.55	R166-5.25	R167-1.30	R168-7.75	R169-3.55	R171-4.55	R174-0.55	R174-9.65
Flow unit	34	35	37	40	43	45	47	47	49	51	52	53	54	55	57	57
Depth (m)	223.1	228.8	241.1	260.0	268.2	281.3	285.5	289.0	299.2	305.7	307.7	312.8	314.5	320.5	324.6	327.4
SiO_2	48.17	47.09	48.38	48.80	48.95	46.26	45.74	45.95	46.25	45.74	45.92	47.01	47.29	46.53	46.89	46.95
TiO_2	1.64	1.66	1.92	1.78	1.84	3.17	3.61	3.22	3.88	4.04	3.98	3.00	3.06	2.23	4.50	4.46
Al_2O_3	10.61	10.63	12.32	10.92	11.12	11.69	13.20	11.89	14.65	14.91	14.63	13.81	14.12	11.11	13.79	13.64
$Fe_2O_3^*$	12.22	12.65	12.50	12.31	12.19	13.93	14.33	14.16	14.04	15.03	14.74	13.31	13.32	12.71	15.11	14.95
MnO	0.17	0.18	0.18	0.17	0.17	0.19	0.20	0.19	0.19	0.20	0.19	0.19	0.19	0.18	0.20	0.20
MgO	16.79	17.67	12.92	15.19	14.80	11.22	8.62	11.20	6.10	6.08	6.30	8.16	7.32	14.17	5.38	5.52
CaO	8.28	8.21	9.55	8.54	8.82	10.34	11.35	10.45	10.70	10.03	10.29	12.01	11.61	10.73	9.69	9.75
Na_2O	1.85	1.71	1.96	1.95	1.97	2.41	2.53	2.38	3.09	2.93	3.01	2.29	2.48	1.88	3.09	3.17
K_2O	0.20	0.14	0.17	0.26	0.23	0.51	0.33	0.42	0.74	0.75	0.77	0.16	0.24	0.16	0.91	0.93
P_2O_5	0.16	0.15	0.18	0.18	0.18	0.32	0.36	0.32	0.35	0.38	0.38	0.32	0.33	0.23	0.56	0.56
Total	100.09	100.09	100.07	100.10	100.27	100.04	100.26	100.19	99.98	100.09	100.20	100.27	99.97	99.92	100.13	100.13
Mg#	0.75	0.75	0.69	0.73	0.73	0.64	0.57	0.64	0.49	0.47	0.48	0.57	0.55	0.71	0.44	0.45
Rb	2.5	1.7	2.3	4.4	2.9	7.2	1.3	3.1	12.2	8.6	10.1	1.3	3.0	1.1	12.7	15.1
Sr	222	209	251	239	253	432	448	427	589	547	568	427	450	325	477	489
Ba	45	27	37	61	69	198	190	203	233	269	269	131	161	143	296	302
La	5	3	5	4	8	16	15	17	17	19	23	16	13	12	27	27
Ce	19	21	20	20	23	43	49	43	47	50	51	42	45	30	62	67
Nb	6.4	6.3	8.5	8.1	7.3	21.5	24.5	21.3	23.4	25.7	26.3	18.9	19.2	12.8	34.1	32.7
Zr	99	99	118	110	109	199	227	204	208	230	225	205	214	148	335	325
Y	21.7	21.3	22.2	20.1	20.9	27.3	30.3	28.0	30.1	31.9	30.7	29.8	30.5	23.1	40.8	41.5
Pb	2	2	1	2	3	3	3	3	4	6	2	3	2	1	4	4
Zn	94	107	107	99	95	118	131	125	110	114	119	118	112	105	144	126
Ga	15	15	18	17	18	21	23	21	25	25	24	21	23	18	26	27
Ni	702	808	461	589	561	329	177	324	83	84	73	154	115	456	67	62
Cr	832	880	586	787	756	842	611	881	116	108	137	391	169	879	97	104
V	199	214	246	212	214	294	327	300	368	355	353	282	269	231	293	293

Table 1. (continued)

	Sample														
	R177-2.60	R180-5.90	R185-3.95	R189-8.50	R193-3.90	R197-0.80	R202-1.40	R208-5.20	R212-0.40	R214-3.00	R215-7.20	R221-4.40	R224-1.75	R229-0.05	R233-3.80	R234-7.40
Flow unit	58	59	62	64	69	70	72	75	76	78	80	88	89	91	96	97
Depth (m)	331.7	342.0	354.5	367.6	378.3	389.4	400.3	415.7	424.1	429.4	433.8	451.2	459.4	472.7	485.4	489.6
SiO_2	43.68	49.09	49.25	43.89	45.04	45.63	49.78	48.67	44.85	49.26	45.39	48.56	49.40	48.03	48.03	47.76
TiO_2	3.96	2.85	2.89	1.16	1.83	1.54	2.74	2.70	1.70	2.72	1.49	2.87	2.73	2.26	2.24	2.37
Al_2O_3	14.39	12.69	13.22	5.99	8.83	7.27	13.32	12.26	8.49	13.04	7.40	14.00	12.90	11.05	11.01	11.45
$Fe_2O_3^*$	15.33	12.53	12.88	13.17	13.52	13.19	12.86	12.36	13.35	12.72	12.86	12.94	12.42	12.59	12.55	12.87
MnO	0.19	0.17	0.18	0.17	0.18	0.18	0.18	0.17	0.18	0.18	0.17	0.18	0.17	0.17	0.17	0.18
MgO	8.21	8.83	7.43	28.25	21.30	23.77	7.40	10.01	22.24	8.40	23.99	7.28	8.89	13.42	14.14	13.02
CaO	9.77	10.49	10.92	5.86	7.25	6.66	10.65	10.61	7.19	10.70	6.86	11.20	10.57	9.43	9.15	9.88
Na_2O	3.24	2.46	2.51	1.15	1.47	1.47	2.40	2.37	1.34	2.32	1.33	2.33	2.39	1.96	1.93	2.09
K_2O	0.84	0.58	0.56	0.08	0.08	0.26	0.49	0.53	0.08	0.44	0.19	0.26	0.47	0.35	0.41	0.28
P_2O_5	0.47	0.31	0.31	0.12	0.19	0.16	0.29	0.31	0.16	0.28	0.15	0.29	0.29	0.23	0.23	0.24
Total	100.08	100.00	100.15	99.84	99.69	100.13	100.11	99.98	99.59	100.06	99.83	99.91	100.23	99.50	99.85	100.13
Mg#	0.541	0.608	0.559	0.825	0.776	0.799	0.559	0.641	0.786	0.592	0.804	0.553	0.612	0.701	0.713	0.690
Rb	15.0	10.1	9.6	0.2	0.8	4.3	7.9	9.2	0.8	6.7	2.8	3.1	7.1	5.6	5.9	4.1
Sr	628	387	388	172	236	205	378	415	222	362	201	386	361	310	300	314
Ba	253	157	172	66	74	79	146	157	68	121	75	99	134	120	110	89
La	20	13	16	3	7	9	10	15	9	14	5	16	14	12	11	10
Ce	58	37	35	18	23	17	29	41	23	30	17	35	37	26	24	30
Nb	28.0	17.0	17.9	6.9	9.9	8.5	14.3	17.0	9.5	14.5	8.1	15.3	15.3	12.7	12.6	12.7
Zr	287	199	197	78	123	102	179	180	119	176	99	191	185	152	147	158
Y	34.8	29.0	28.8	13.2	19.3	16.3	28.0	25.0	17.9	27.6	15.8	30.0	27.9	23.6	23.0	24.6
Pb	3	4	2	4	2	3	2	3	3	3	2	3	2	3	1	3
Zn	129	110	110	103	117	102	110	110	112	111	106	112	106	112	110	111
Ga	26	20	21	9	15	12	21	20	14	20	12	23	21	18	17	18
Ni	151	207	134	1321	930	1030	130	255	961	174	1133	112	199	457	568	419
Cr	116	413	295	1730	1221	1641	209	486	1120	371	1494	249	433	849	982	807
V	267	238	277	143	189	165	267	224	189	267	169	253	243	221	217	221

Table 1. (continued)

	Sample															
	R243-8.40	R246-5.20	R250-0.00	R251-3.90	R259-0.75	R286-0.90	R287-3.15	R291-0.05	R298-0.50	R303-3.00	R311-0.70	R315-3.55	R319-1.30	R322-3.50	R323-2.10	R327-2.80
Flow unit	103	105	106	107	109	118	119	120	125	126	131	132	137	138	139	141
Depth (m)	513.3	520.1	526.6	530.9	542.2	590.1	594.1	603.8	615.7	623.3	645.0	658.2	669.4	677.6	680.3	689.8
SiO_2	46.51	47.55	47.38	50.28	46.39	47.21	49.31	48.91	48.75	46.53	49.51	47.85	46.82	46.95	50.01	49.77
TiO_2	1.76	2.13	2.27	2.50	1.74	1.95	2.83	2.31	2.30	1.78	2.26	2.38	2.12	2.11	2.67	2.65
Al_2O_3	8.65	10.21	10.82	13.07	8.61	9.51	13.40	12.08	11.91	8.83	12.45	10.41	10.11	10.09	13.53	13.34
$Fe_2O_3^*$	12.41	12.51	12.77	12.34	12.72	12.59	12.73	12.19	12.46	12.60	12.59	12.88	12.97	12.95	12.44	12.34
MnO	0.17	0.17	0.18	0.17	0.17	0.17	0.18	0.17	0.17	0.17	0.18	0.18	0.18	0.18	0.17	0.17
MgO	20.01	15.61	14.64	8.30	20.60	18.25	7.72	11.23	11.71	20.33	10.14	15.28	16.60	16.56	7.38	7.79
CaO	8.17	8.76	9.25	10.42	7.61	8.07	10.99	10.74	9.99	7.72	10.19	8.55	8.58	8.60	10.98	11.07
Na_2O	1.63	1.91	1.99	2.34	1.54	1.82	2.33	2.02	2.05	1.67	2.18	1.98	1.80	1.83	2.34	2.32
K_2O	0.24	0.42	0.28	0.48	0.25	0.33	0.38	0.33	0.35	0.28	0.27	0.43	0.28	0.28	0.36	0.38
P_2O_5	0.17	0.22	0.23	0.26	0.17	0.20	0.29	0.22	0.22	0.18	0.21	0.25	0.20	0.21	0.26	0.26
Total	99.73	99.49	99.80	100.15	99.80	100.10	100.16	100.19	99.91	100.10	99.98	100.19	99.66	99.76	100.14	100.09
Mg#	0.780	0.733	0.716	0.597	0.781	0.761	0.572	0.670	0.674	0.780	0.639	0.723	0.738	0.738	0.566	0.581
Rb	3.7	6.9	3.9	7.6	4.1	5.4	5.9	4.5	4.6	4.6	4.3	7.2	4.1	5.1	5.3	6.1
Sr	236	301	317	350	228	257	361	320	303	245	295	308	273	247	346	355
Ba	89	118	125	125	77	92	121	123	95	92	84	125	91	98	101	127
La	7	13	11	13	6	10	13	8	10	9	5	12	8	13	9	10
Ce	19	25	29	32	21	24	34	28	27	25	21	34	26	20	32	31
Nb	9.4	13.2	13.5	14.9	9.4	10.8	16.5	12.2	12.1	10.1	10.7	13.7	11.5	9.8	13.8	14.5
Zr	114	148	147	164	114	131	192	145	146	120	142	161	136	125	170	171
Y	18.4	22.1	23.1	25.8	18.0	19.3	21.0	23.2	23.5	18.1	24.3	24.1	21.2	19.5	27.8	27.4
Pb	1	4	3	2	3	1	2	4	2	4	4	2	3	3	2	2
Zn	105	110	108	105	109	106	116	103	107	103	106	112	113	107	112	107
Ga	14	17	18	21	14	15	21	20	19	14	20	18	15	17	22	23
Ni	832	606	541	174	917	762	130	321	385	897	194	615	707	649	113	120
Cr	1359	955	846	365	1434	942	347	675	670	1275	549	842	1017	976	251	332
V	183	213	213	244	187	203	283	227	239	175	254	218	213	205	245	269

Table 1. (continued)

	Sample															
	R329-6.50	R331-1.90	R333-2.10	R340-5.15	R347-6.35	R350-2.45	R356-1.45	R362-0.55	R365-0.05	R371-0.30	R374-5.90	R379-3.80	R382-4.35	R385-5.55	R395-1.00	R399-4.30
Flow unit	142	143	144	147	152	153	155	158	159	164	165	167	169	170	173	176
Depth (m)	696.2	699.0	704.6	720.3	738.7	747.4	759.7	775.6	781.2	797.4	808.2	821.4	829.2	835.6	855.9	869.1
SiO_2	49.77	46.02	46.93	47.76	45.68	50.29	49.49	46.18	46.18	47.31	46.16	49.55	46.54	49.77	49.05	50.14
TiO_2	2.64	1.69	2.09	2.20	1.55	2.62	2.60	1.75	1.66	1.95	1.64	2.18	1.76	2.35	2.56	2.61
Al_2O_3	13.32	8.58	10.48	10.76	7.99	13.03	12.76	8.39	8.02	9.64	8.36	12.45	8.61	13.02	12.58	12.87
$Fe_2O_3^*$	12.34	12.63	12.68	12.55	12.62	12.36	12.58	12.61	12.60	12.60	12.39	12.77	12.52	12.67	12.86	12.10
MnO	0.18	0.17	0.17	0.17	0.17	0.17	0.18	0.17	0.17	0.17	0.17	0.18	0.17	0.18	0.18	0.17
MgO	7.78	21.64	16.60	15.38	22.91	7.56	8.39	21.09	22.41	17.79	21.64	9.93	20.78	8.25	9.29	8.59
CaO	11.07	7.21	8.70	8.96	6.86	11.05	10.79	7.39	7.10	8.10	7.24	10.44	7.33	10.77	10.72	10.65
Na_2O	2.33	1.46	1.71	1.88	1.49	2.33	2.33	1.60	1.47	1.73	1.48	2.24	1.70	2.31	2.21	2.33
K_2O	0.38	0.15	0.19	0.29	0.21	0.47	0.39	0.24	0.21	0.33	0.24	0.32	0.28	0.37	0.35	0.42
P_2O_5	0.26	0.17	0.20	0.23	0.15	0.26	0.26	0.17	0.16	0.20	0.16	0.20	0.18	0.23	0.25	0.26
Total	100.07	99.71	99.76	100.18	99.63	100.14	99.77	99.58	99.98	99.81	99.48	100.26	99.87	99.92	100.05	100.13
Mg#	0.581	0.790	0.742	0.730	0.800	0.574	0.595	0.786	0.797	0.757	0.794	0.631	0.785	0.589	0.614	0.610
Rb	5.5	1.4	2.1	4.5	3.1	7.9	5.8	3.6	3.6	5.5	4.4	4.3	4.6	5.4	5.3	6.7
Sr	327	218	277	293	206	353	341	231	217	262	224	275	216	308	335	329
Ba	119	61	99	110	83	126	108	86	74	94	74	81	103	103	119	115
La	11	6	10	10	8	15	11	5	6	7	7	7	10	10	12	8
Ce	26	19	25	25	18	31	34	19	24	25	20	27	21	27	34	30
Nb	13.1	9.5	12.1	13.4	8.6	14.1	14.1	9.2	9.3	12.2	9.0	10.9	9.7	11.5	14.4	14.0
Zr	159	108	140	144	101	170	168	113	109	128	105	133	118	147	167	171
Y	25.2	17.5	21.5	21.6	15.6	26.4	26.6	17.8	16.6	19.8	16.7	23.6	19.2	24.6	25.3	26.9
Pb	3	3	1	3	3	3	4	3	4	4	1	2	1	3	3	3
Zn	109	112	111	110	108	107	109	104	108	108	99	112	104	105	113	106
Ga	20	14	16	17	13	21	20	14	13	16	13	20	16	20	22	20
Ni	165	1009	686	623	1091	107	134	956	1074	792	936	199	899	150	163	179
Cr	466	1122	886	839	1337	326	421	1331	1371	983	1403	521	1259	363	449	480
V	245	187	213	222	178	248	253	183	176	202	177	237	191	249	250	250

Table 1. (continued)

	Sample													
	R401-4.90	R413-1.40	R419-5.30	R424-9.30	R428-2.70	R431-3.70	R434-7.90	R442-2.10	R446-2.40	R452-3.90	R457-4.30	R463-6.00	R464-7.10	R466-5.00
Flow unit	177.00	189.00	190.00	196.00	197.00	200.00	203.00	208.00	211.00	218.00	220.00	224.00	225.00	227.00
Depth (m)	875.36	910.25	922.57	939.15	946.31	954.85	965.24	983.92	994.68	1009.47	1024.62	1043.70	1047.14	1052.44
SiO_2	49.26	48.17	49.78	49.68	50.23	45.52	48.28	46.65	48.37	50.03	49.00	48.81	48.77	49.17
TiO_2	2.19	2.03	2.17	2.16	2.53	1.31	1.99	1.63	2.18	2.60	2.43	2.41	2.35	2.56
Al_2O_3	12.10	10.40	12.19	12.16	12.92	7.04	10.56	8.49	10.46	13.03	11.99	11.75	11.89	11.92
$Fe_2O_3^*$	12.76	12.50	12.35	12.31	12.33	12.76	12.79	12.65	12.57	12.57	12.55	12.70	12.49	12.77
MnO	0.18	0.17	0.17	0.17	0.17	0.17	0.17	0.17	0.17	0.18	0.17	0.17	0.17	0.17
MgO	10.75	15.92	10.83	10.77	8.21	25.58	15.08	21.37	15.16	8.40	11.04	11.79	11.67	11.05
CaO	10.08	8.68	9.96	9.94	10.77	6.04	8.58	7.09	8.57	10.46	9.69	9.51	9.69	9.67
Na_2O	2.09	1.91	2.18	2.15	2.28	1.37	1.96	1.56	1.96	2.29	2.33	2.12	2.30	2.25
K_2O	0.32	0.35	0.33	0.33	0.43	0.20	0.33	0.25	0.41	0.44	0.48	0.44	0.43	0.36
P_2O_5	0.21	0.20	0.21	0.21	0.24	0.14	0.20	0.17	0.24	0.26	0.26	0.26	0.25	0.27
Total	99.94	100.33	100.17	99.89	100.12	100.12	99.93	100.03	100.09	100.26	99.94	99.96	100.01	100.19
Mg#	0.65	0.74	0.66	0.66	0.59	0.82	0.72	0.79	0.73	0.60	0.66	0.67	0.67	0.66
Rb	5.0	5.7	5.2	4.9	7.2	2.8	5.2	4.0	7.0	7.5	7.7	7.5	6.9	5.5
Sr	288	270	275	294	325	167	255	201	270	341	336	331	331	341
Ba	98	99	76	104	109	55	86	72	105	133	134	121	104	121
La	8	7	8	8	7	5	12	7	12	11	12	12	9	11
Ce	28	24	26	24	27	16	21	17	31	33	34	30	35	31
Nb	10.5	11.2	10.8	10.6	12.9	6.8	9.9	8.8	13.5	14.9	14.6	14.1	13.7	15.3
Zr	139	135	137	135	164	86	131	108	160	168	167	161	161	171
Y	23.0	21.2	23.2	22.8	26.0	13.8	22.0	17.4	23.8	26.3	24.5	24.1	22.7	25.3
Pb	3	1	3	3	1	3	3	3	3	4	3	2	2	2
Zn	108	107	109	100	111	107	104	108	117	112	111	110	115	112
Ga	18	16	18	20	22	12	18	13	18	21	20	21	19	20
Ni	221	644	370	189	155	1353	513	997	601	167	285	322	318	310
Cr	610	900	562	436	420	1286	751	1398	939	348	669	712	713	661
V	242	213	231	220	267	151	221	189	221	259	242	234	228	240

$Fe_2O_3^*$ is total Fe expressed as Fe_2O_3. Mg# is Mg/(Mg+Fe) after adjusting Fe^3/total Fe to 0.1.

Table 2. Data for USGS standard BHVO-1 and the HSDP standard Kil-1919

	BHVO-1	HSDP						HSDP	HSDP
		Split 1	Split 2	Split 3	Split 4	Split 5	Split 6	Average	S. D.
SiO_2	49.58	49.72	49.70	49.91	49.91	49.81	49.70	49.81	0.090
TiO_2	2.740	2.767	2.756	2.770	2.761	2.761	2.756	2.763	0.005
Al_2O_3	13.61	13.68	13.72	13.75	13.76	13.73	13.69	13.73	0.028
$Fe_2O_3^*$	12.17	12.11	12.09	12.09	12.16	12.06	12.07	12.10	0.033
MnO	0.17	0.17	0.17	0.17	0.17	0.17	0.17	0.17	0.001
MgO	7.09	6.95	6.91	6.91	6.93	6.94	6.90	6.93	0.016
CaO	11.35	11.39	11.39	11.40	11.41	11.42	11.38	11.40	0.012
Na_2O	2.40	2.49	2.54	2.49	2.49	2.47	2.55	2.50	0.023
K_2O	0.522	0.527	0.527	0.530	0.529	0.525	0.527	0.528	0.002
P_2O_5	0.272	0.275	0.272	0.279	0.273	0.270	0.274	0.274	0.003
Total	99.90	100.08	100.08	100.30	100.39	100.16	100.02	100.20	
Mg#	0.562	0.558	0.557	0.557	0.556	0.559	0.557	0.558	
Rb	9.2	9.0	8.9	9.2	9.2	8.8	-	9.0	0.16
Sr	388	397	398	397	398	401	-	398.2	1.33
Nb	19.4	19.6	19.4	19.1	19.9	19.5	-	19.5	0.26
Zr	191	187	187	186	188	185	-	186.8	1.18
Y	24.6	25.0	25.2	25.0	25.2	25.3	-	25.1	0.12
Pb	3	3	1	3	4	2	-	2.7	0.99
Zn	113	110	109	111	111	109	-	109.7	0.83
Ga	21	21	21	22	21	21	-	21.2	0.37
Ni	126	104	101	104	108	112	-	105.6	3.72
Cr	284	267	265	272	270	265	-	267.8	2.75
V	285	289	285	289	290	286	-	287.7	1.65
Ce	36	32	33	32	33	33	-	32.5	0.46
Ba	139	137	135	135	133	137	-	135.3	1.43
La	16	12	11	12	12	14	-	12.3	1.05

0.70 (assuming a K_D of 0.3 [*Roeder and Emslie*, 1970]) which translates to an MgO content in the parental magmas of about 14.7 wt % (Figure 8). On the other hand, the most forsteritic olivine phenocryst identified in these lavas is $Fo_{90.8}$ [*Garcia*, this issue], implying that more MgO-rich, picritic magmas may be the ultimate parental magmas. An olivine of this composition will be in equilibrium with a melt having an FeO/MgO of 0.60 (Figure 8). This corresponds to an MgO content of 16.9 wt. percent in this parental, and possibly primary magma. Picritic parental magmas with similar MgO contents have been proposed for Kilauea [*Clague et al.*, 1991], and for submarine lavas from the southwest rift zone of Mauna Loa [*Garcia et al.*, 1995]. It follows from such a parental composition that the numerous lavas with MgO greater than 17 wt % must have accumulated olivine.

There is little compositional evidence of multiply saturated lavas that have differentiated beyond olivine control through crystallization of plagioclase and clinopyroxene in addition to olivine at lower temperatures. Flow unit 27 (R117) is an exception: it has the lowest MgO content (6.8%), unusually high Al_2O_3 and low total iron abundances and may possibly have accumulated plagioclase. Such lavas are very rare on Mauna Loa. The rarity of "differentiated" lavas [*Wright and Fiske*, 1971] and the dominance of olivine control is a

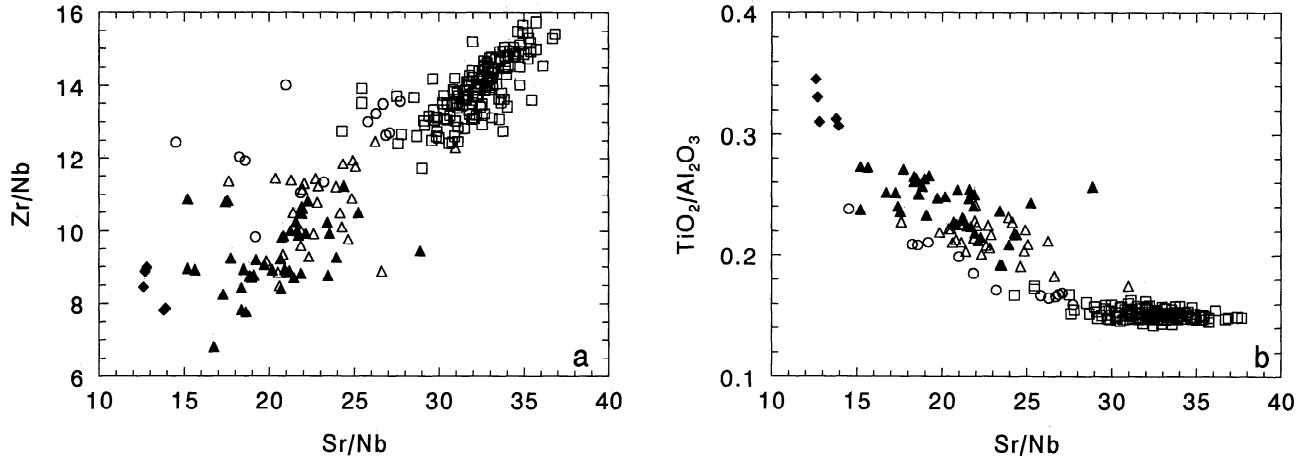

Figure 1. Discriminant diagrams for Mauna Loa and Mauna Kea lavas. (a) Zr/Nb versus Sr/Nb. (b) TiO_2/Al_2O_3 versus Sr/Nb. Historical Mauna Loa tholeiitic lavas are shown as open squares; submarine Mauna Kea tholeiites as open circles; tholeiitic and alkalic lavas from the Hamakua Volcanics of Mauna Kea as open and solid triangles, respectively; and high-Fe Hamakua basalts as solid diamonds. The Mauna Loa data are from *Rhodes* [1983, 1988, 1995] and *Rhodes and Hart* [1995], and the Mauna Kea data are from *Frey et al.* [1990, 1991] and *Yang and Frey* [1994].

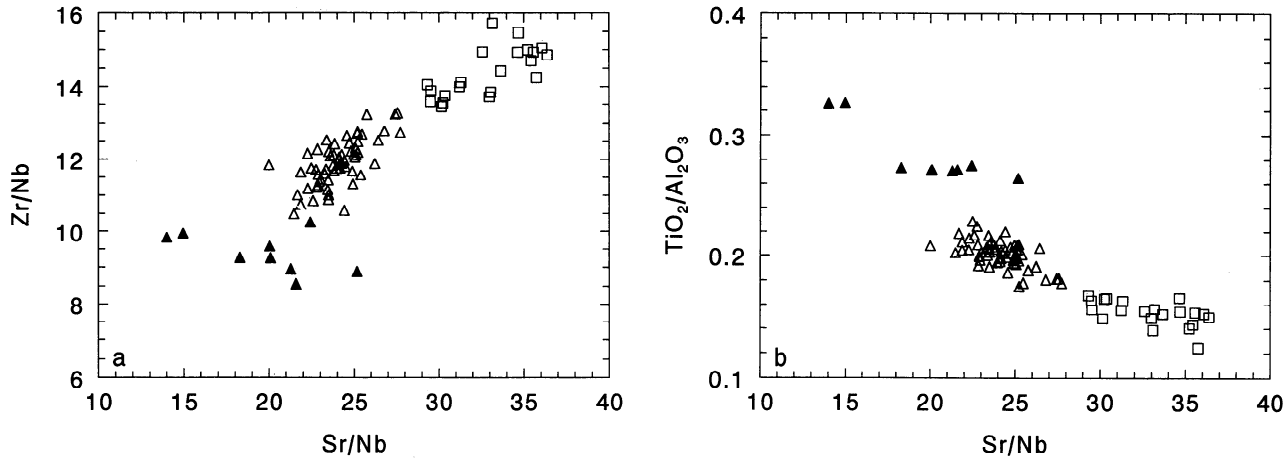

Figure 2. (a) Zr/Nb and (b) TiO_2/Al_2O_3 versus Sr/Nb in basaltic lavas recovered by the Hawaiian Scientific Drilling Project. Basalts inferred to have erupted on Mauna Loa are shown as open squares. Tholeiites inferred to have erupted on Mauna Kea are shown as open triangles, and alkali basalts as solid triangles.

characteristic of historical and prehistoric Mauna Loa lavas [*Wright*, 1971; *Rhodes*, 1983, 1988, also unpublished data, 1995] and has been attributed by *Rhodes* [1988, 1995] and *Rhodes and Hart* [1995] to the continual replenishment of a shallow, steady state magma reservoir. Most of these "steady state" magmas, however, tend to cluster at the low- MgO end of the olivine-control trend, with MgO abundances between 6.7 and 8.0 wt % [*Rhodes*, 1988, 1995]. With the exception of flow unit 27, none of the HSDP Mauna Loa samples fall within this range. Most are olivine-rich, with MgO > 9%, and many contain over 14% (Figures 6-9) and are therefore picritic [*Rhodes*, 1995]. There is no obvious systematic MgO distribution with depth (Figure 10). The MgO contents fluctuate widely from picritic magmas to MgO-rich basalts with 9-12% MgO. The range is similar to that of the historical picritic eruptions of 1852 and 1868. Such high-MgO abundances are, however, not common for subaerial Mauna Loa lavas. Within the historical record they account for only 7% of the volume [*Lockwood and Lipman*, 1987] and *Powers* [1955] estimated that they comprise only about 15% of the volume of the Mauna Loa and Kilauea volcanic shields. Picrites, however, are characteristic and prevalent among the possibly 100-200 ka lavas erupted along the submarine portion of Mauna Loa's southwest rift zone [*Garcia et al.*, 1995]. Recent studies propose that high-MgO and picritic Mauna Loa magmas are the typical products of the deeper portions of a stratified magma column and that they may tend to be erupted subaerially during periods of high magma supply [*Garcia et al.*, 1995; *Rhodes*, 1995].

The ratios of Zr/Nb and Sr/Nb are relatively constant in the Mauna Loa lavas, averaging 14.4 and 32.9 compared with 13.8 and 31.9 in historical lavas [*Rhodes and Hart*, 1995]. There are, however, systematic variations with depth in such ratios as Sr/Y, Zr/Y, and Nb/Y. All of these ratios decrease gradually with increasing depth to about 230 m, beyond which they increase again down to 280 m (Figure 11). Systematic fluctuations in these ratios have also been recorded in historical Mauna Loa lavas within as little as 141 years [*Rhodes and Hart*, 1995] and in successive prehistoric flows exposed in the walls of Mokuoweoweo, the summit caldera [*Sparks*, 1990].

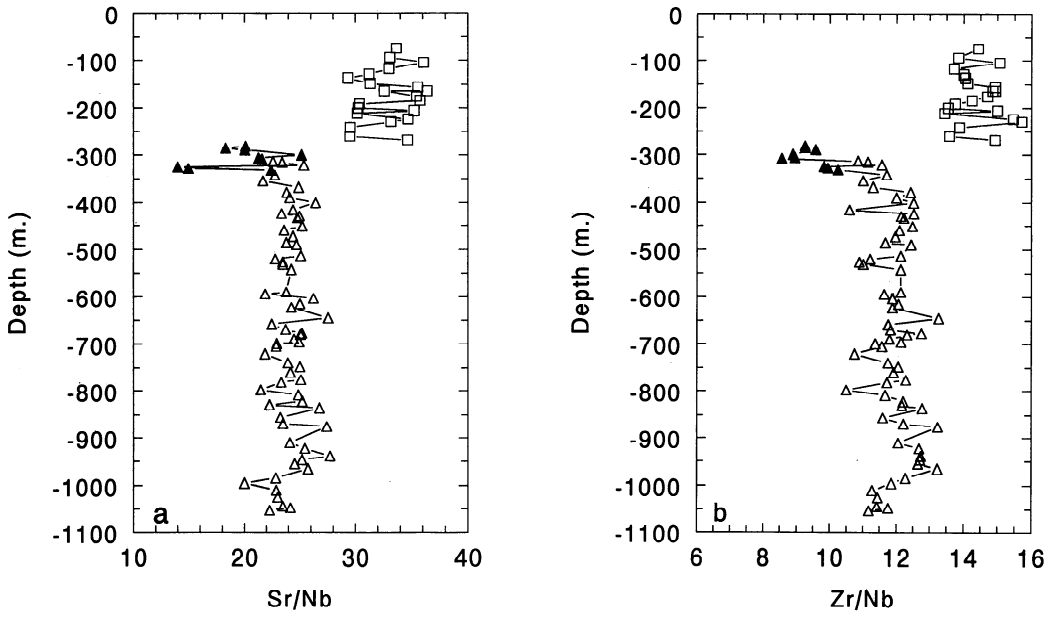

Figure 3. Variations of (a) Sr/Nb and (b) Zr/Nb with depth in lavas from the Hawaii Scientific Drill Hole. The symbols are the same as in Figure 2.

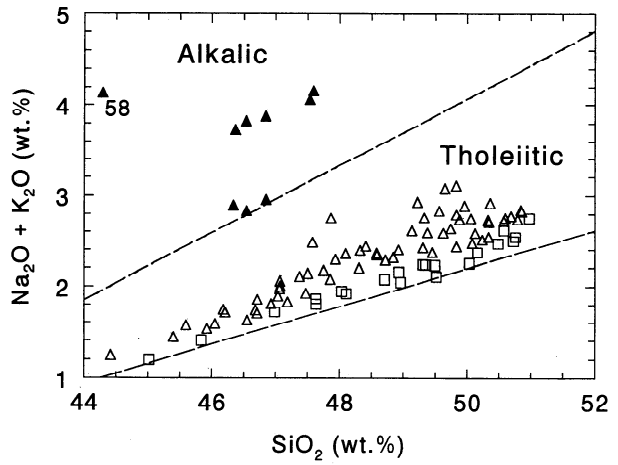

Figure 4. Total alkali - silica diagram for samples from the Hawaii Scientific Drill Hole. Symbols are the same as in Figure 2. The thick dashed line separating the fields for alkalic and tholeiitic lavas is taken from *Carmichael et al.* [1974, Figure 8-9] and is given by total alkali = SiO_2 x 0.37-14.43. The thin dashed line is a regression line for historical Mauna Loa lavas [*Rhodes and Hart,* 1995] and is shown for reference.

Sr/Y ratios in the HSDP Mauna Loa tholeiites range from values that compare closely with average historical lavas in the upper flows to values that are considerably lower than the most depleted historical lavas (the summit 1880 eruption) at depths of around 200 m. These values are lower than in any historical, or relatively young prehistoric lava (<10 kyr) and compare closely with the lowest values recorded in lavas that are thought to be older than 100 kyr [*Lipman,* 1995]. Such lavas include flows from the subaerial Ninole and Kahuku basalts and from submarine lavas of the southwest rift zone [*Lipman et al.,* 1990; *Rhodes,* 1993, also unpublished data, 1995; *Garcia et al.,* 1995]. Similar temporal variations are also seen in chondrite-normalized La/Yb ratios [*Yang et al.,* this issue] which range from 4.7 in the uppermost flow to 4.0 at 223 m then increase to 4.5 at the base of the Mauna Loa flows at 268 m. In contrast with Sr/Y, the La/Yb ratios are all within the range found in historical lavas [*Rhodes and Hart,* 1995].

Mauna Kea Lavas

As noted above, basaltic flows with the geochemical characteristics of Mauna Kea samples extend from a depth of 280 m to the bottom of the hole at 1056 m. Between 280 and 340 m there is a series of alkalic basalt flows that are interlayered with tholeiitic flows, basaltic conglomerates and soil horizons. The interlayered tholeiites, between 310 and 323 m, deviate from the main Mauna Kea tholeiitic trend (Figs. 4, 6a, 8). Below 340 m. all of the flows are tholeiitic (Figs. 4, 5) but the flows immediately beneath the alkalic flows, between 340 and 425 m, also deviate from the main tholeiitic trend. Ar/Ar dating yields an age of 201 ka for flow unit 49, one of the uppermost alkalic flows at 299 m; similarly flow unit 58, the lowest of the alkalic flows (332 m) yields an age of 241 ka. A tholeiite (flow unit 211) near the bottom of the hole is dated at 447 ka [*Sharp et al.,* this issue].

Alkalic Basalts

The deepest alkali basalt flow (flow unit 58 at 332 m.) is strongly alkalic with low SiO_2 (Figures 4, 5, and 6a) and is a basanitoid in composition [*Yang et al.,* this issue]. It is overlain by a moderately alkalic flow, which in turn is overlain by 13 m of a number of thin tholeiite flows. These are overlain by 30 m of more alkalic flows (flow units 45-52). The lower three of these five flows are moderately alkalic, while the upper two are only weakly alkalic (Figures 4 and 5). There are frequent soil horizons and rubble zones interlayered with these flows, indicating that the eruption rate was probably very low and intermittent.

All of the alkalic flows are distinctly higher in TiO_2, total iron as Fe_2O_3, P_2O_5, Rb, Sr, Ba, Nb, Zr, Ce, La, Y, V, and Ga than the tholeiites at corresponding MgO values (Figures 6-8). By definition, of course, SiO_2 is lower, and Na_2O and K_2O are higher. The K_2O and Rb abundances are highly variable, however, and may reflect varying degrees of alteration. Concentrations of Ni and Cr at a given MgO content are similar to those of the tholeiites, but the actual abundances tend to cluster at the low-MgO end of the trend because of more extensive fractionation.

Figure 8 clearly illustrates the higher iron content of the alkalic magmas, which is also reflected in Figure 9, where the linear trend for high-MgO alkali basalts is distinct from that of the tholeiites and intersects the abscissa at a value corresponding to $Fo_{85.5}$. This is considerably less forsteritic than the value found for the Mauna Kea tholeiites ($Fo_{88.4}$, see below) but is close to the maximum forsterite content of olivines of Fo_{85-86} reported for the alkalic basalts [*Garcia,* this issue]. This implies that melts with FeO/MgO ratios of about 1.0, similar to flow units 45 and 47 which each have about 11.2% MgO (Figure 8), are suitable parental magma compositions for the alkali basalts. The other alkali basalts could have differentiated from melts with similar FeO/MgO ratios. Their lower CaO and Al_2O_3 abundances at a given MgO content (Figures 6-9) suggest that differentiation was multiphased involving plagioclase and clinopyroxene . The most evolved alkalic basalt (flow unit 57), with MgO of about 5.5%, has notably lower V abundances (Figure 7e), perhaps implying that it has also fractionated opaques. Total iron and TiO_2 are not, however, significantly lower in this flow.

Tholeiitic Lavas

The tholeiitic lavas that are interlayered with the alkalic basalts and immediately underlie them to a depth of 425 m deviate somewhat from the main Mauna Kea tholeiitic trend. These lavas are distinguished by one or more of the following characteristics relative to the

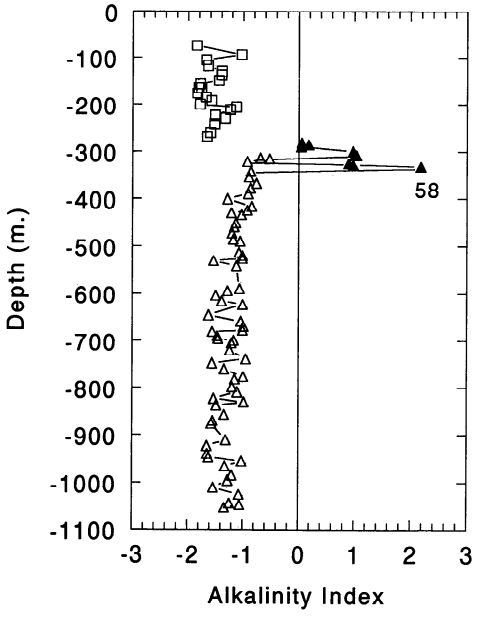

Figure 5. Variation of the alkalinity index with depth in samples from the Hawaii Scientific Drill Hole. Symbols are the same as in Figure 2. The alkalinity index reflects the departure from the line separating alkalic and tholeiitic lavas in Figure 4 (alkalinity index = total alkali - (SiO_2 x 0.37-14.43)). Tholeiitic lavas have negative values, whereas alkalic lavas are positive.

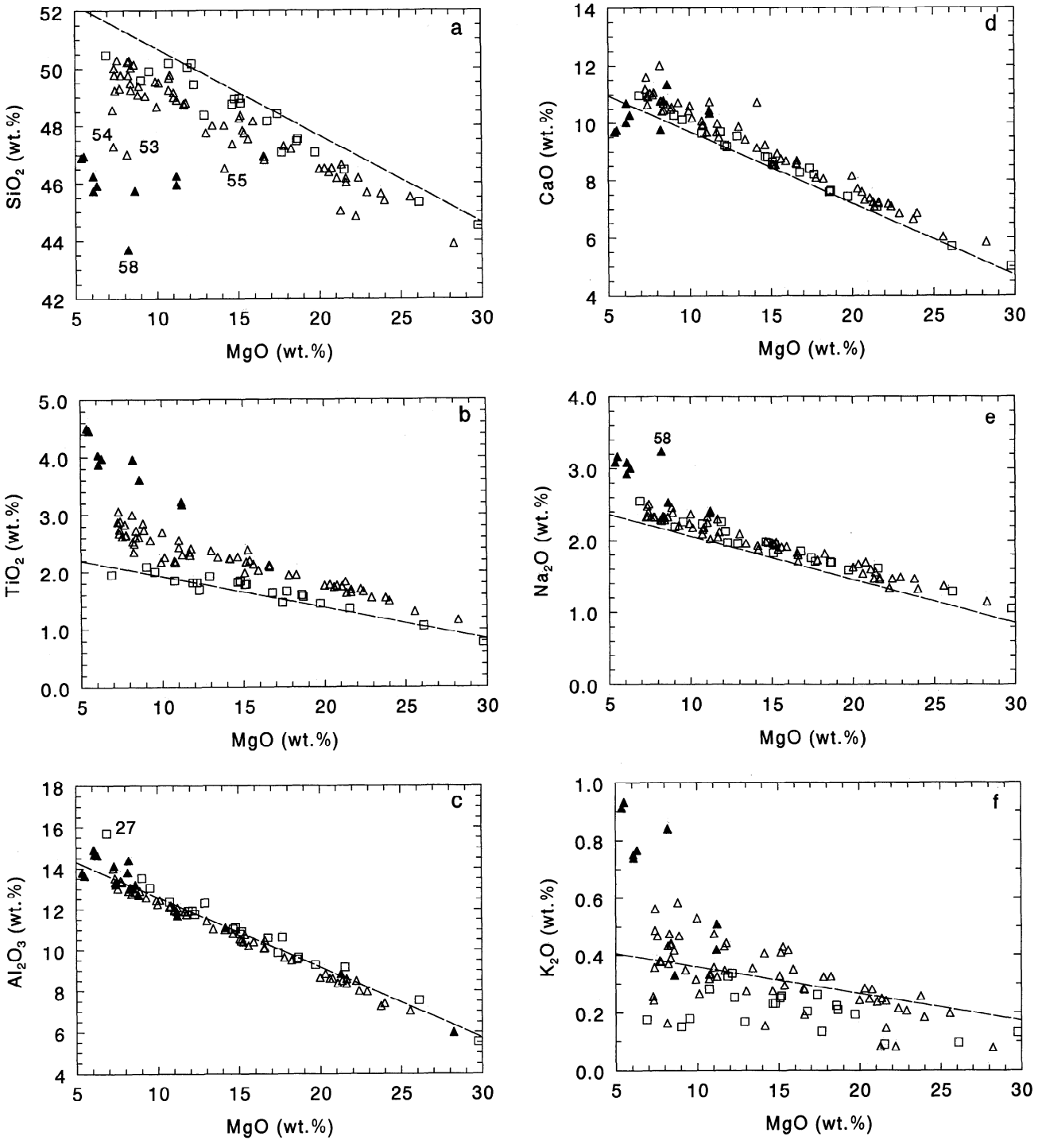

Figure 6. Abundances of major elements (a) SiO_2, (b) TiO_2, (c) Al_2O_3, (d) CaO, (e) Na_2O and (f) K_2O versus MgO content in lavas from the Hawaii Scientific Drill Hole. The symbols are the same as in Figure 2. Regression lines for historical Mauna Loa lavas are shown as dashed lines for reference.

other Mauna Kea tholeiites: high total alkalis at a given SiO_2 content (Figure 4), lower SiO_2 (Figure 6a) or higher FeO (Figure 8) at a given MgO content. The distinction is somewhat arbitrary as only flow units 53 and 54, interlayered between the alkali basalts, possess all of these attributes. Nonetheless, the fact that these tholeiite flows are spatially associated with the alkali basalts in the upper 100 m of the Mauna Kea stratigraphic column raises the question as to whether or not they are tending toward alkalic compositions. Compared with tholeiites lower in the stratigraphic column they tend also to be slightly higher, but not distinctly so, in incompatible elements (TiO_2, P_2O_5, Nb, Zr, Y, Sr, Ba, Ce) at a given MgO content (Figures 6 and 7). One exception is flow unit 75 at 416 m. It is unusually high in Sr (Figures 7b and 11a) and the light rare earth elements [*Yang et al.*, this issue].

K_2O and Rb abundances are extremely low in many of these deviant samples (Figure 6f), with correspondingly low K_2O/P_2O_5 ratios (< 1), perhaps indicating extensive alteration. *Lipman et al.* [1990] suggest that in addition to loss of K_2O and Rb, SiO_2 may also be leached out of samples through extensive alteration and that Fe_2O_3 can

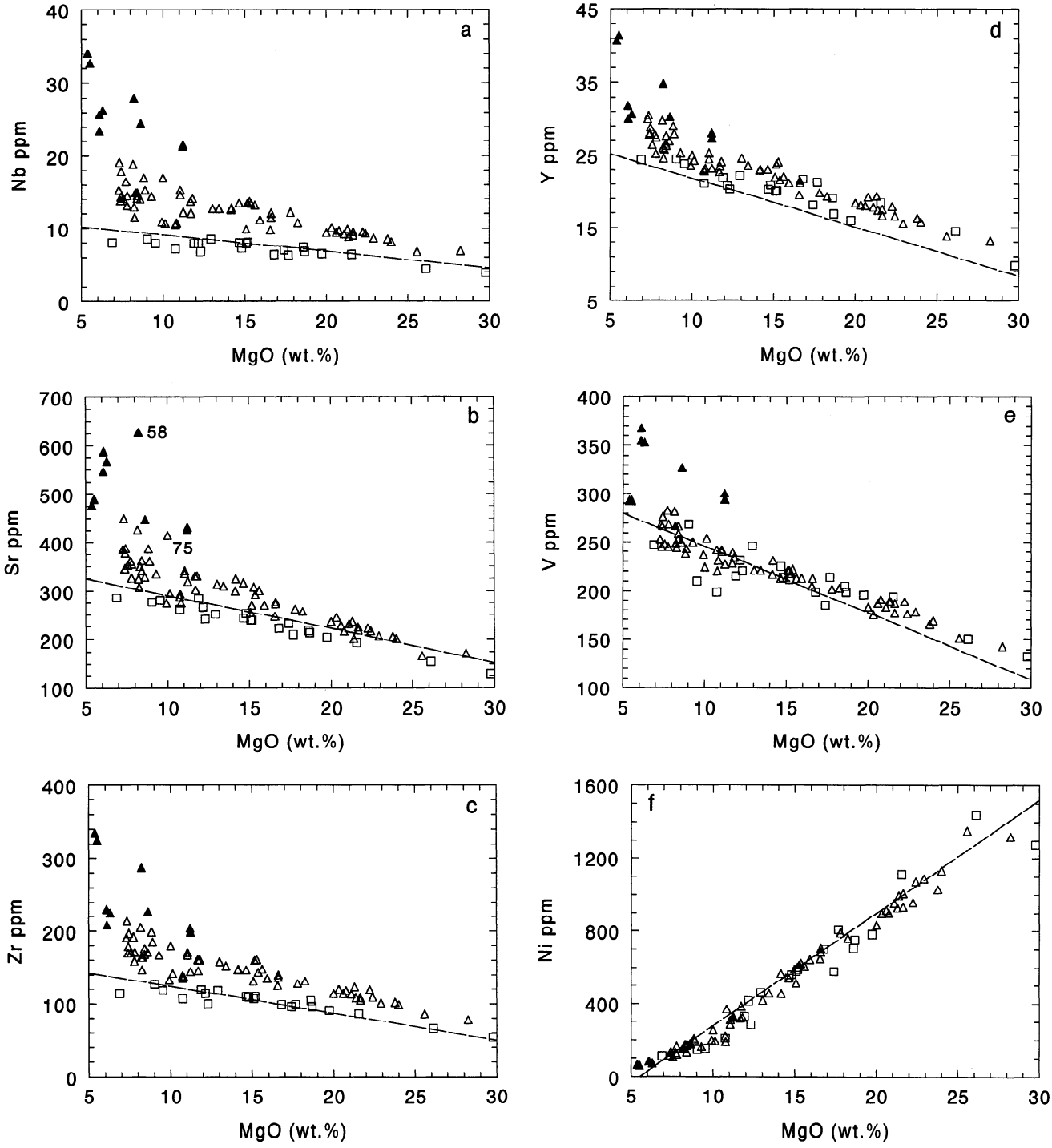

Figure 7. Abundances of trace elements (a) Nb, (b) Sr, (c) Zr, (d) Y, (e) V and (f) Ni versus MgO content in lavas from the Hawaii Scientific Drill Hole. The symbols are the same as in Figure 2. Regression lines for historical Mauna Loa lavas are shown as dashed lines for reference.

be concentrated. If leaching operated on these flows during periods of infrequent eruption and long surface exposure, some of the characteristics of these samples could be an artifact of alteration. On the other hand, there are flows deeper in the stratigraphic column that also have low K_2O/P_2O_5 ratios but do not exhibit similar deviations from the main tholeiitic trend.

It is clear from Figures 6-9 that these deviant tholeiites have closer affinities with the other Mauna Kea tholeiites than they do with the alkalic basalts. This is also readily apparent from Figure 2, where they show Sr/Nb, Zr/Nb, and TiO_2/Al_2O_3 ratios that fall within the fields of the Mauna Kea tholeiites.

As noted above, the Mauna Kea tholeiites are consistently higher in incompatible elements than the Mauna Loa tholeiites at comparable MgO contents. They are also slightly higher in FeO at a given MgO content than the Mauna Loa lavas. Consequently, they exhibit different trends on plots of FeO versus MgO and Al/(Mg+Fe) versus Mg/(Mg+Fe) (Figures 8 and 9). In Figure 9, the intersection of the Mauna Kea tholeiite trend with the abscissa is at $Fo_{88.4}$, compared with

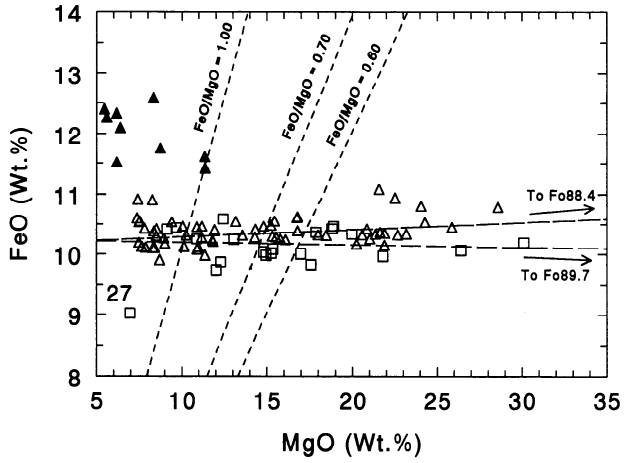

Figure 8. FeO-MgO relationships in lavas from the Hawaii Scientific Drill Hole. The symbols are the same as in Figure 2. FeO is calculated from total iron by assuming that 10% of the iron is present as Fe^{3+}. Regression lines for the tholeiitic Mauna Loa and Mauna Kea lavas are shown as long-dashed lines. They intersect the compositional trend for olivines at FeO-MgO values corresponding to $Fo_{89.7}$ and $Fo_{88.4}$, respectively. The oblique, short-dashed lines reflect the FeO/MgO of melts in equilibrium (assuming K_D = 0.3 [*Roeder and Emslie*, 1970]) with the most forsteritic olivines in the lavas. These correspond to $Fo_{90.8}$ in the Mauna Loa lavas, $Fo_{89.5}$ in the Mauna Kea tholeiites, and $Fo_{85.5}$ in the alkalic Mauna Kea lavas [*Garcia*, this issue]. The intersection of these lines with the regression lines for the data provides an estimate of the composition of the parental magma from which these olivines crystallized. These correspond to a maximum MgO content for an alkalic parental magma of about 11.2 wt %, about 14.7 wt % in a parental Mauna Kea tholeiite, and about 16.9 wt % in a parental Mauna Loa tholeiite.

an olivine composition of $Fo_{88.9}$ estimated from the regression of FeO versus MgO (Fiure. 8). $Fo_{88.4}$ olivine compositions should be in equilibrium with a parental melt with an FeO/MgO of about 0.78 (assuming K_D of 0.3 [*Roeder and Emslie*, 1970]), which in the Mauna Kea tholeiites corresponds to an MgO content of about 12.3 wt %. The most forsteritic olivine phenocrysts (as distinct from xenocrysts) identified in these lavas is $Fo_{89.5}$ [*Garcia*, this issue], which can be taken to imply a parental magma with an FeO/MgO of about 0.7. Figure 8 shows that such magmas in the Mauna Kea tholeiites would have an MgO content of about 14.9 wt %, substantially less

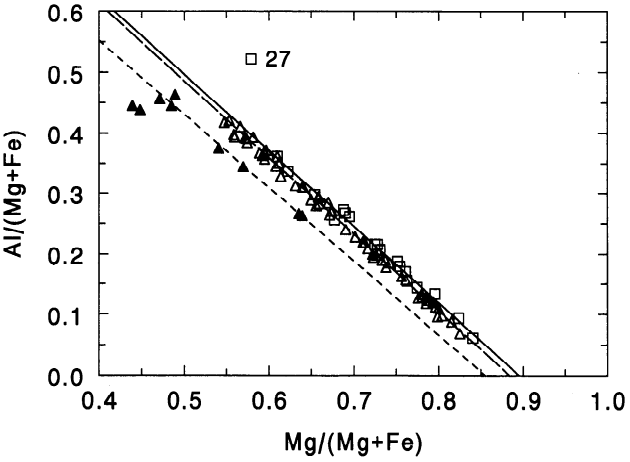

Figure 9. Al/(Mg+Fe) versus Mg/(Mg+Fe) in lavas from the Hawaii Scientific Drill Hole. As in Figure 8, FeO is calculated from total iron by assuming that 10% of the iron is present as Fe^{3+}. The symbols are the same as in Figure 2. Regression lines are shown for the Mauna Loa tholeiites, the Mauna Kea tholeiites and the alkalic Mauna Kea basalts. They intersect the abscissa at Mg/(Mg+Fe) values of 0.89, 0.88 and 0.85, respectively.

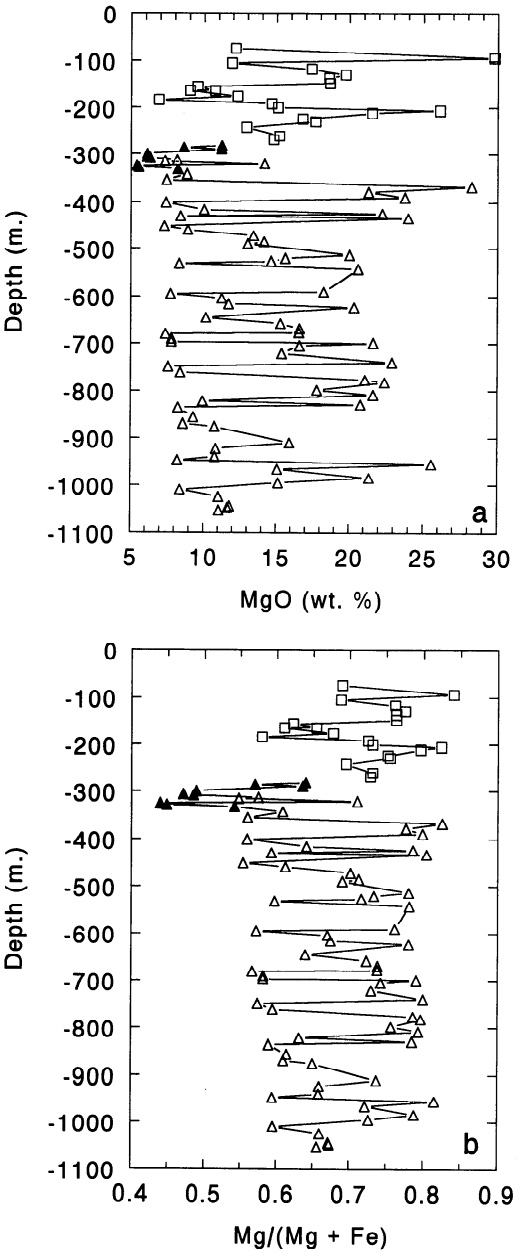

Figure 10. Variations of (a) MgO content and (b) Mg/(Mg+Fe) with depth in lavas from the Hawaii Scientific Drill Hole. Symbols are the same as in Figure. 2.

than the estimated MgO content of 16.9 wt % for the Mauna Loa parental magma. It is, however, close to the MgO content of picritic glasses recovered from the submarine flanks of Kilauea [*Clague et al.*, 1991]. Flows with MgO contents above 14.9 wt % must have accumulated olivine.

There are abundant picritic flows (MgO > 14%) amongst the Mauna Kea tholeiites (Figure 10). There is no obvious distribution with depth, with the implication that picritic magmas were relatively common throughout the almost 200 ka [*Sharpe et al.*, this issue] of eruptive history reflected by the tholeiites. Unlike the overlying Mauna Loa lavas, there are basaltic flows with more "normal" MgO contents, typically in the range of 7.3 to 10.0 wt. percent. There are, however, none lower than this, implying that there are no lavas that have differentiated substantially beyond olivine-control through multi phase crystallization, despite the presence of clinopyroxene and plagioclase phenocrysts. Previously, I have interpreted this phenome-

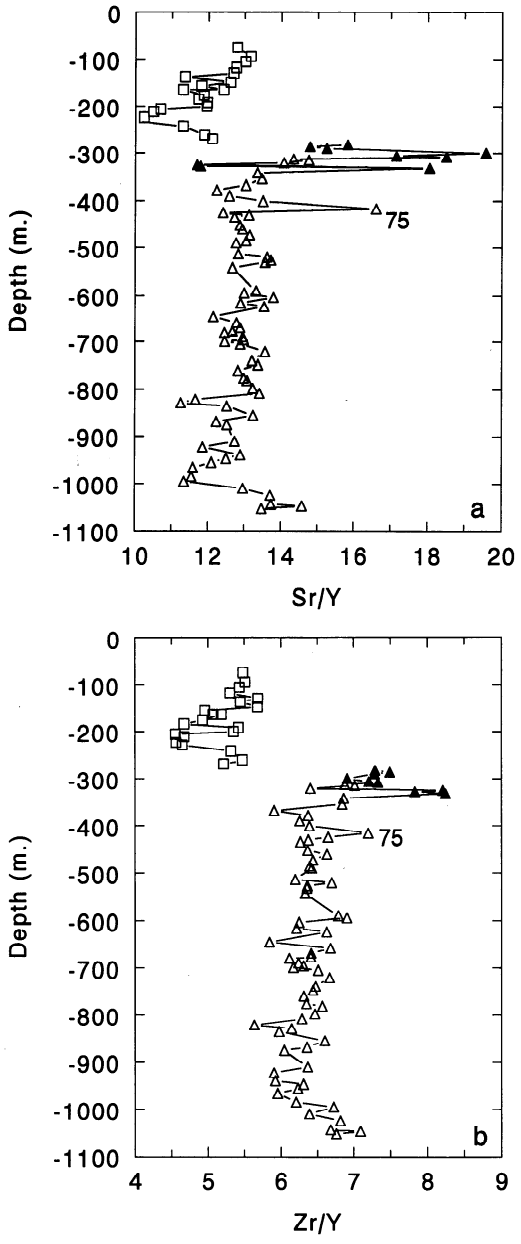

Figure 11. Variations of (a) Sr/Y and (b) Zr/Y with depth in lavas from the Hawaii Scientific Drill Hole. Symbols are the same as in Figure 2.

non, where lavas are "perched" at the low-MgO end of an olivine-control trend, as evidence for continuing magma replenishment in a quasi steady state open system [*Rhodes*, 1988, 1995; *Rhodes and Hart*, 1995]. The MgO content of these "normal" basalts gradually increases with increasing depth, from a low of about 7% at around 400-500 m to about 8-9% at 900-1000 m. This is more clearly seen in a progressive increase in the minimum Mg value with depth from about 0.55 to 0.60 (Figure10b).

The ratios Zr/Nb and Sr/Nb, although changing slightly [*Yang et al.*, this issue], remain approximately constant at about 11-13 and 22-28, respectively, throughout the 675 m of the tholeiitic record (Figure 3). Given that on other Hawaiian volcanoes these ratios broadly correlate with Sr and Pb isotopes [e.g., *Frey and Rhodes*, 1993; *Frey et al.*, 1994; *Roden et al.*, 1994; *Rhodes and Hart*, 1995; *Kurz et al.*, 1995; *Chen et al.*, 1996], it seems likely that the source of these tholeiites has probably remained constant over this time period. Ratios of other incompatible elements (e.g., Sr/Y, Zr/Y, and Nb/Y), however, do vary with increasing depth (Fig. 11). Although there is considerable "noise" in the data, these ratios progressively decrease from about 400 to 1000 m, after which they abruptly increase. *Yang et al.* [this issue] report similar systematic fluctuations in La/Yb.

Implications for Mauna Loa

The available record of Mauna Loa's eruptive history is essentially bi modal. Most of the surface area is covered by historical lava flows and prehistoric lavas that are younger in age than 30 ka, most of these being less than 10 ka [*Lockwood and Lipman*, 1987; *Lipman*, 1995; *Lockwood*, 1995]. Older lavas are exposed in fault scarps of the Ninole Hills, the Kahuku and Kealakekua Pali's, and the submarine portion of the southwest rift zone. Although not precise, available dates indicate that these flows range in age between 100 and200 ka and that the submarine lavas are probably even older [*Lipman et al.*, 1990; *Garcia et al.*, 1995; *Lipman*, 1995]. This hiatus in the eruptive record is critical, because it appears that the supply and eruption of magma on Mauna Loa may have declined dramatically at some time in this period [*Lipman*, 1995].

On the basis of an isostatic subsidence rate of 2.2-2.6 mm/yr for the island of Hawaii, modified to account for eustatic sea level curves and constrained by a few isotopic ages, *Lipman and Moore* [this issue] and *Lipman* [1995] suggest that Mauna Loa flows in the HSDP core range in age from about 10 ka to a maximum of about 80-100 ka. Consequently, the HSDP core provides an extremely important link between these two previously sampled populations, shedding light on the magmatic evolution of Mauna Loa over this critical intervening period.

Of first concern is why the Mauna Loa portion of the HSDP core is dominated by picrites and high-MgO basalts? As noted earlier, these are rare amongst historical and prehistoric (< 31 ka) lavas. They are extremely abundant, however, in submarine lavas from the submarine extension of the Kahuku fault scarp along the southwest rift zone, and common, but less abundant, in the subaerial segment of the scarp [*Garcia et al.*, 1995]. *Garcia et al.* [1995] and *Rhodes* [1995] explain this distribution by suggesting that Mauna Loa's magma column is density-stratified from picritic magmas at depth to low-MgO (6.8-8.0) magmas in the shallow summit reservoir and that picrites are preferentially erupted along the submarine section of the rift zone. Additionally, *Rhodes* [1995] proposes that during periods of high magma supply, picritic magmas rise in the magma column resulting in the infrequent subaerial picritic eruptions. These interpretations are consistent with a cyclical model of eruptive activity proposed by *Lockwood* [1995], based on detailed geologic mapping and radiocarbon dating. A cycle begins with a period of near-continuous summit lava lake activity and summit overflows, presumably reflecting high magma supply rates and high-level magma storage. The end of this period is triggered when a large rift zone eruption (possibly picritic?) lowers the magma column and results in caldera collapse, shifting surface activity from the summit to frequent eruptions along the two rift zones.

If these interpretations are valid, they imply that, in the 10-100 kyr represented by HSDP cores of Mauna Loa flows, either there has been continued tapping of picritic magmas from deep within the magma column, or that there has been a sustained high magma supply rate throughout this entire period. Neither alternative appears plausible. This is because the HSDP lavas are subaerial [*Stolper et al.*, this issue], whereas the picritic lavas on the southwest rift zone are pillowed, and were erupted in a submarine environment. In other words, the HSDP flows are probably supplied from higher in the magma column. Furthermore, there are occasional "normal" basalts (7-8% MgO) interlayered with the submarine picrites, but (with the exception of flow unit 27) not with the HSDP lavas (Figure 12).

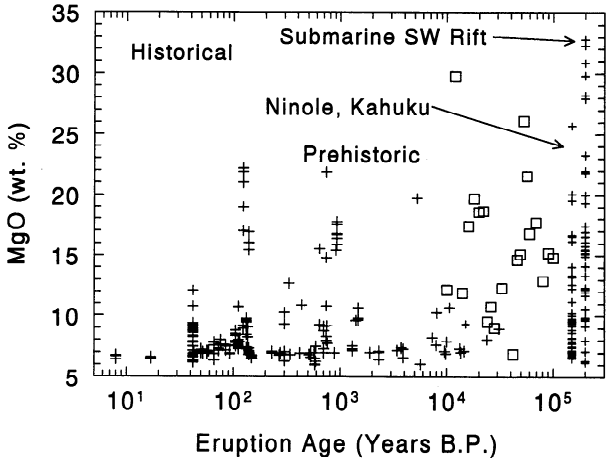

Figure 12. MgO content versus age for Mauna Loa lavas. Historical and prehistoric radiocarbon dated lavas are shown as crosses, and the HSDP samples are shown as open squares. The Kahuku and Ninole basalts (also crosses) have been assigned an arbitrary age of 150 ka., whereas the lavas from the submarine southwest rift zone have been assigned an age of 200 ka. Ages assigned to the HSDP samples are only approximate and are extrapolated from sea-level curves [*Lipman*, 1995; *Lipman and Moore*, this issue]. Data are from *Rhodes* [1983, 1988, 1995, also unpublished data, 1995]; *Lipman et al.*, [1990] and *Rhodes and Hart* [1995].

Figure 12, although by no means complete, shows that there appear to be brief periods in Mauna Loa's eruptive history when picrites and high-MgO basalts are erupted. Picrites are not common elsewhere on the volcano between 10-30 ka, the period of overlap between radiocarbon dated samples [*Lockwood*, 1995] and the HSDP core. As noted above, however, subaerial samples corresponding to this time period are not abundant and sampling may well be biased.

A more plausible explanation for the overwhelming abundance of picrites and high-MgO basalts in the Mauna Loa portion of the HSDP core is that the flows sampled by the core may not be representative of those erupted on the rest of the volcano during this period. The drill site is far removed from the currently active segment of Mauna Loa's northeast rift zone. Consequently, it is probable that only hot, highly mobile, large-volume flows get as far as Hilo Bay. These are likely to be picritic or high-MgO in composition. For example, using the glass-based geothermometer of *Montierth et al.* [1995], picritic flows with 16.9 wt % MgO will have an eruption temperature of about 1400°C compared with about 1170-1200°C for more normal basalts with 7-8 wt % MgO.

As noted earlier, ratios of incompatible elements involving Nb (e.g., Zr/Nb, Sr/Nb, La/Nb, Nb/Y) correlate broadly with $^{87}Sr/^{86}Sr$ and $^{206}Pb/^{204}Pb$ in Hawaiian lavas, and reflect variations in source components in the Hawaiian plume. Examination of Figure 13a shows that Zr/Nb, although fluctuating, has remained within a characteristic range of 12-16 over much of Mauna Loa's accessible eruptive record. The major exceptions are the old (>200 ka?) lavas erupted along the submarine extension of the Kahuku fault along the southwest rift zone. These lavas exhibit a wide range in Zr/Nb, from values that are similar to subaerial Mauna Loa lavas to lower values similar to those of Kilauea and Mauna Kea [*Rhodes et al.*, 1989; *Frey et al.*, 1990,1991; *Frey and Rhodes*, 1993; *Rhodes*, 1993]. This decrease in Zr/Nb is accompanied by changes in the isotopic ratios of Sr and Pb, with the implication that the source of Mauna Loa magmas at that time contained components that were closer to the present-day source of Kilauea [*Kurz and Kammer*, 1991; *Rhodes*, 1993; *Kurz et al.*, 1995; *Garcia et al.*, 1995]. The Zr/Nb (and Sr/Nb) ratios of the HSDP lavas are within the range for historical and young (<30 ka) prehistoric Mauna Loa lavas (Figure 13a). They are at the high end of this range (13.5-15), which is characteristic of the more depleted historical lavas erupted around 1880-1887 during a period of high eruptive activity [*Rhodes and Hart*, 1995] and also of contemporaneous (10-30 ka) lavas erupted elsewhere on the volcano. The implications are that the source for HSDP lavas has remained essentially Mauna Loa-like over the 10 to 100 kyr eruptive record provided by these samples.

Unlike Zr/Nb and other ratios involving Nb, other incompatible element ratios (e.g., K/Y, Sr/Y, La/Yb) do not remain relatively constant over time. There are systematic temporal variations in historical lavas and in prehistoric lavas exposed in the walls of the summit caldera [*Rhodes and Hart*, 1995; *Sparks*, 1990]. There is also considerable variation within the prehistoric record (Figure 13b). *Rhodes and Hart* [1995] suggest that these changes are a reflection of varying magma supply rates. Low ratios result when a relatively depleted parental magma is dominating the supply to the magma system. This depleted parental magma results from more extensive melting, with the consequence that magma supply and eruption rates are correspondingly high. If this interpretation is valid, then it appears that magma supply rates were low on Mauna Loa between about 200-5,000 years., a possible exception being between about 700 and 1500 years (an interval corresponding roughly with period 3 of *Lockwood and Lipman* [1987], a time when eruption rates were comparatively high).

The HSDP Mauna Loa lavas have relatively low ratios of Sr/Y and Zr/Y (Figures 11 and 13b). Chondrite-normalized La/Yb ratios between 2.7 and 3.1 [*Yang et al*, this issue] are also at the low-end of the range for historical lavas [*Rhodes and Hart*, 1995]. K/Y cannot be evaluated because of alteration. The upper flows have values that

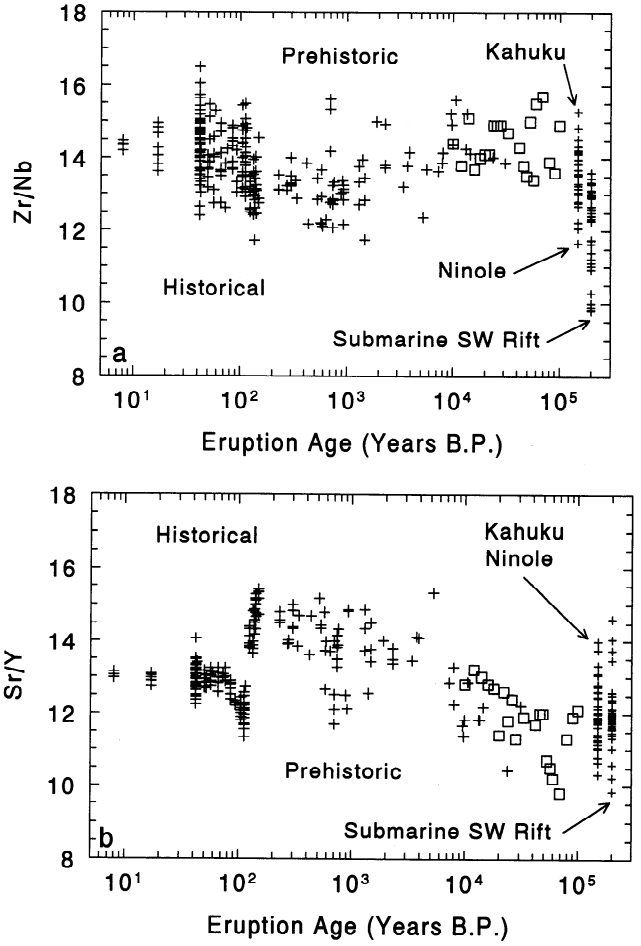

Figure 13. (a) Zr/Nb and (b) Sr/Y versus age for Mauna Loa lavas. Symbols, assumptions, and sources of data are the same as in Figure 12.

correspond with the lower values found in the historical and prehistoric record. With increasing depth these ratios become progressively lower (Figure 11), until at a depth of about 200-230 m, corresponding roughly with an age of 50-80 ka [*Lipman and Moore*, this issue], unusually low values of Sr/Y and Zr/Y are attained. From 230 to 280 m, at the base of the Mauna Loa section, these values again rise to more "normal" but still low values. The low Sr/Y and Zr/Y values in the Mauna Loa lavas between 200 and 230 m are not found in the historical record [*Rhodes and Hart*, 1995] or in young (<10 ka) prehistoric lavas (Figure 13b). They are found, however, among old (>100 ka?) prehistoric lavas. If there is a connection between these ratios and eruption and magma supply rates, then the implications are that throughout the interval represented by the HSDP Mauna Loa core (about 10-100 ka) these rates have been relatively high. Between 1843 and 1887, when these ratios attained their lowest values in the historical record (Figure 13b), the eruption rate averaged 47 x 10^6 m^3/yr [*Lockwood and Lipman*, 1987], almost twice the long-term magma supply rate of 26 x 10^6 m^3/yr proposed by *Lipman* [1995] for Mauna Loa. This implies that between 10 and 50 ka, the eruption and magma supply rates may have been similar to, or somewhat higher than, modern rates and that they were probably even higher than this between 50 and 80 ka. Thus, the HSDP core samples encompass a critical period in Mauna Loa's magmatic history, and may provide a record of the radical decline in magmatic output recently proposed by *Lipman* [1995]. Conversely, it could be a sampling effect. If, as I suggest above, picrites are also preferentially erupted during periods of high magma supply, and only hot, mobile picritic flows make it as far as Hilo Bay, then picritic magmas with low Sr/Y and Zr/Y ratios are perhaps to be expected in the HSDP core. If this is the case, there could be lavas of this age elsewhere on the volcano with compositions that reflect low magma supply rates

Conclusions

1. Element ratios involving Nb and TiO_2, such as Zr/Nb, Sr/Nb, and TiO_2/Al_2O_3, provide useful discriminants between lavas erupted on Mauna Loa and Mauna Kea volcanoes. They also contribute to discrimination between alkalic and tholeiitic lavas.

2. The Hawaii Scientific Drilling Project has sampled flows from both Mauna Loa and Mauna Kea volcanoes. The upper 280 m of the core consists of tholeiitic Mauna Loa flows. Beneath these, between 280 and 340 m, is a 60-m-thick zone of alkalic basalts and tholeiites that correlate with the postshield Hamakua Volcanics of Mauna Kea. Beneath the Hamakua Volcanics, from 340 m to the bottom of the hole at 1056 m, is a 675 m-thick section of shield-building Mauna Kea tholeiites.

3.The Mauna Loa and Mauna Kea tholeiites are broadly similar in composition, but the Mauna Kea tholeiites contain higher abundances of incompatible elements at a given MgO content than the tholeiites from Mauna Loa; they are also slightly lower in SiO_2 and total iron. The Mauna Kea parental magmas are more iron-rich and are estimated to contain about 15 wt % MgO, whereas parental Mauna Loa magmas are estimated to contain about 17 wt %t MgO. Picrites are abundant throughout both the Mauna Loa and Mauna Kea segments of the core. Those with more than 15-17 wt % MgO have undoubtedly accumulated olivine.

4. Among the picritic and high-MgO Mauna Kea tholeiites are more "normal" tholeiites with MgO between 7.3 and 10.0 wt %. These magmas are "perched" at the end of an olivine-control trend and may be indicative of a continuously replenished magma reservoir during this period of Mauna Kea's activity, similar to the current magma reservoir proposed for Mauna Loa [*Rhodes*, 1988, 1995]. The MgO content of these tholeiites increases with depth, perhaps indicating a decline in the magma supply rate over time.

5. There are no "normal" low-MgO tholeiites among the Mauna Loa lavas, only picrites and high-MgO tholeiites. No special significance for the eruptive record is attached to this. Rather it is proposed that the abundance of these lavas reflects the fact that only large-volume, hot, mobile flows are likely to reach Hilo Bay from the northeast rift zone.

6. The inferred eruption ages of the Mauna Loa tholeiites (10-100 ka [*Lipman and Moore*, this issue]) are critical for evaluating the eruptive history of Mauna Loa at a time when magma supplies may have been drastically reduced [*Lipman*, 1995]. Lavas erupted over this period help to fill the gap between historical and young prehistoric lavas (mostly <10 ka) and other older lavas (100-200 ka?) exposed in fault scarps and along the submarine extension of the southwest rift zone.

7. Ratios such as Zr/Nb and Sr/Nb have remained roughly constant, within the range for historical and young (< 31 ka) prehistoric lavas. There are no low ratios similar to those found among old (> 200 ka?) submarine lavas from the southwest rift zone [*Rhodes*, 1993; *Kurz et al.*, 1995]. This can be taken to imply that the source components for Mauna Loa magmas in the Hawaiian plume have remained essentially constant over the time period (10-100 ka?) reflected by the HSDP cores and are similar to those for modern lavas.

8. Systematic changes in incompatible element ratios (e.g., Sr/Y, Zr/Y, La/Yb) are interpreted to be sensitive to the melting history and therefore to reflect the supply and eruption of magma. If valid, this implies that between 10 and 50 ka the supply of magma to Mauna Loa was comparable with the highest modern rates, and that between 50-80 ka the magma supply rate was probably considerably higher.

Acknowledgments. Special thanks to D. DePaolo, E. Stolper, and D. Thomas for initiating and bringing this project to fruition. Thoughtful reviews that improved the clarity and content of the paper were provided by M. B. Baker, F. A. Frey, H. R. Naslund, and C. Rhodes. J. Sweeney devised the sample washing procedures and provided assistance with the XRF analyses. The XRF facilities at UMass are ably maintained by P. Dawson.

References

Budahn, J. R., and R. A. Schmitt, Petrogenetic modeling of Hawaiian tholeiitic basalts: A geochemical approach, *Geochim. Cosmochim. Acta, 49*, 67-87, 1985.

Carmichael, I. S. E., F. J. Turner, and F. Verhoogen, *Igneous Petrology*, McGraw-Hill, New York, 1974.

Chen, C.-Y., F. A. Frey, J. M. Rhodes, and R. M. Easton, Temporal geochemical evolution of Kilauea Volcano: Comparison of Hilina and Puna basalt, in *Earth Processes: Reading the Isotopic Code, Geophys. Monogr. Ser.*, vol. 95, edited by A. Basu and S. R. Hart, pp. 161-182, AGU, Washington, D.C., 1996.

Clague, D. A., W. S. Weber, and J. E. Dixon, Picritic glasses from Hawaii, *Nature, 353*, 553-556, 1991.

Frey, F. A., and J. M. Rhodes, Intershield geochemical differences among Hawaiian volcanoes: implications for source compositions, melting process and magma ascent paths, *Philos. Trans. R. Soc. London A, 342*, 121-136, 1993.

Frey, F. A., M. O. Garcia, W. S. Wise, A. Kennedy, P. Gurriet, and F. Albarede, Evolution of Mauna Kea volcano, Hawaii: Petrologic and geochemical constraints on postshield volcanism, *J. Geophys. Res., 95*, 1271-1300, 1990.

Frey, F. A., W. S. Wise, M. O. Garcia, H. West, S.-T. Kwon, and A. Kennedy, Evolution of Mauna Kea volcano, Hawaii: Petrogenesis of tholeiitic and alkalic basalts, *J. Geophys. Res., 96*, 14,347-14,375, 1991.

Frey, F. A., M. O. Garcia, and M. F. Roden, Geochemical characteristics of Koolau volcano: Implications of intershield geochemical differences among Hawaiian volcanoes, *Geochim. Cosmochim. Acta, 58*, 1441-1462, 1994.

Garcia, M. O. Petrography and olivine and glass chemistry of lavas from the Hawaii Scientific Drilling Project, *J. Geophys. Res.*, this issue.

Garcia, M. O., T. Hulsebosch and J. M. Rhodes, Olivine-rich submarine basalts from the southwest rift zone of Mauna Loa volcano: Implications for magmatic processes and geochemical evolution, in *Mauna Loa Revealed: Structure, Composition, History, and Hazards, Geophys. Monogr. Ser.*, vol. 92, edited by J. M. Rhodes and J. P. Lockwood, pp. 219-239, AGU, Washington, D.C., 1995.

Irvine, T. N., Rocks whose composition is determined by crystal accumulation and sorting, in *The Evolution of the Igneous Rocks Fiftieth Anniversary Perspectives*, edited by H. S. Yoder Jr., pp. 245-306, Princeton Univ. Press, Princeton, N. J., 1979.

Kurtz, M. D., and D. P. Kammer, Isotopic evolution of Mauna Loa volcano, *Earth Planet. Sci. Lett., 103*, 257-269, 1991.

Kurz, M. D., T. C. Kenna, D. P. Kammer, J. M. Rhodes, and M. O. Garcia, Isotopic evolution of Mauna Loa Volcano: a view from the submarine southwest rift zone, in *Mauna Loa Revealed: Structure, Composition, History, and Hazards, Geophys. Monogr. Ser.*, vol. 92, edited by J. M. Rhodes and J. P. Lockwood, pp. 289-306, AGU, Washington, D.C., 1995.

Lipman, P. W., and J. G. Moore, Mauna Loa lava accumulation rates at the Hilo drill site: Formation of lava deltas during a period of declining overall volcanic growth, *J. Geophys. Res.* this issue).

Lipman, P. W., J. M. Rhodes, and M. A. Lanphere, The Ninole Basalt-Implications for the structural evolution of Mauna Loa volcano, Hawaii, *Bull. Volcanol., 53*, 1-19, 1990.

Lipman, P. W., Declining growth of Mauna Loa during the last 100,000 years: Rates of lava accumulation vs. gravitational subsidence, in *Mauna Loa Revealed: Structure, Composition, History, and Hazards, Geophys. Monogr. Ser.*, vol. 92, edited by J. M. Rhodes and J. P. Lockwood, pp. 45-80, AGU, Washington, D.C., 1995.

Lockwood, J. P., Mauna Loa eruptive history-The preliminary radiocarbon record, in *Mauna Loa Revealed: Structure, Composition, History, and Hazards, Geophys. Monogr. Ser.*, vol. 92, edited by J. M. Rhodes and J. P. Lockwood, pp. 81-94, AGU, Washington, D.C., 1995.

Lockwood, J. P. and P. W. Lipman, Holocene eruptive history of Mauna Loa Volcano, *U.S Geol. Surv. Prof. Pap., 1350*, 509-535, 1987.

Montierth, C., A. D. Johnston, and K. V. Cashman, An empirical glass-composition-based geothermometer for Mauna Loa lavas, in *Mauna Loa Revealed: Structure, Composition, History, and Hazards, Geophys. Monogr. Ser.*, vol. 92, edited by J. M. Rhodes and J. P. Lockwood, pp. 207-217, AGU, Washington, D.C., 1995.

Norrish, K., and B. W. Chappell, X-ray fluorescent spectrography, in *Physical Methods in Determinative Mineralogy*, edited by J. Zussman, pp. 161-214, Academic, San Diego, Calif., 1967.

Norrish, K., and J. T. Hutton, An accurate X-ray Spectrographic method for the analysis of a wide range of geological samples, *Geochim. Cosmochim. Acta, 33*, 431-454, 1969.

O'Nions, R. K., P. J. Hamilton, and N. M. Evensen, Variations in $^{143}Nd/^{144}Nd$ and $^{87}Sr/^{86}Sr$ ratios in oceanic basalts, *Earth Planet. Sci. Lett., 34*, 13-22, 1977.

Powers, H. A., Composition and origin of basaltic magmas on the Hawaiian islands, *Geochim. Cosmochim. Acta, 7*, 77-107, 1955.

Reynolds, R. C., Jr., Estimation of mass absorption coefficients by Compton scattering: Improvements and extension of the method, *Am. Mineral., 52*, 1493-1502, 1967.

Rhodes, J. M., Homogeneity of lava flows: Chemical data for historic Mauna Loa eruptions, *Proc. Lunar. Planet. Sci. Conf. 13th, Part 2, J. Geophys. Res., 88 suppl.*, A869-A879, 1983.

Rhodes, J. M., Geochemistry of the 1984 Mauna Loa eruption: Implications for magma storage and supply, *J. Geophys. Res., 93*, 4453-4466, 1988.

Rhodes, J. M., Geochemical constraints on the magmatic evolution of Mauna Loa Volcano, Hawaii (abstract), *Eos Trans AGU, 74(43)*, Fall Meet. Suppl., 629, 1993.

Rhodes, J. M., The 1852 and 1868 Mauna Loa Picrite eruptions: Clues to parental magma compositions and the magmatic plumbing system, in *Mauna Loa Revealed: Structure, Composition, History, and Hazards, Geophys. Monogr. Ser.*, vol. 92, edited by J. M. Rhodes and J. P. Lockwood, pp. 241-262, AGU, Washington, D.C., 1995.

Rhodes, J. M., and S. R. Hart, Episodic trace element and isotopic variations in historical Mauna Loa lavas: Implications for magma and plume dynamics, in *Mauna Loa Revealed: Structure, Composition, History, and Hazards, Geophys. Monogr. Ser.*, vol. 92, edited by J. M. Rhodes and J. P. Lockwood, pp. 263-288, AGU, Washington, D.C., 1995.

Rhodes, J. M., K. P. Wenz, C. A. Neal, J. W. Sparks, and J. P. Lockwood, Geochemical evidence for invasion of Kilauea's plumbing system by Mauna Loa magma, *Nature, 337*, 257-260, 1989.

Roden, M. F., T. Trull, S. R. Hart, and F. A. Frey, New He, Sr, Nd and Pb isotopic constraints on the constitution of the Hawaiian Plume: Results from Koolau volcano, Oahu, Hawaii, *Geochim. Cosmochim. Acta, 58*, 1431-1440, 1994.

Roeder P. L., and R. F. Emslie, Olivine liquid equilibrium, *Contrib. Mineral. Petrol., 29*, 275-289, 1970.

Sharp, W. D., B. D. Turin, P. R. Renne, and M. A. Lanphere, The $^{40}Ar/^{39}Ar$ and K/Ar dating of lavas from the Hilo 1-km core hole, Hawaii Scientific Drilling Project, *J. Geopys. Res.*, this issue.

Sparks, J. W., Long-term compositional and eruptive behavior of Mauna Loa Volcano: evidence from prehistoric caldera basalts, Ph.D. thesis, Univ.of Mass., Amherst, 1990.

Stolper, E. M., D. M. Thomas and, D. J. DePaolo, Introduction to special section: Hawaii Scientific Drilling Project, *J. Geopys. Res.* this issue.

Tatsumoto, M., Isotopic composition of lead in oceanic basalt and its implication to mantle evolution, *Earth Planet. Sci. Lett., 38*, 13-29, 1978.

Thomas, D. M., F. L. Paillet, and M. E. Conrad, Hydrogeology of the Hawaii Scientific Drilling Project borehole KP-1,2, Groundwater geochemistry and regional flow patterns, *J. Geopys. Res.*, this issue.

Tilling, R. I., T. L. Wright, and J. R. Millard Jr., Trace-element chemistry of Kilauea and Mauna Loa lava in space and time: A reconnaissance, *U.S. Geol. Surv. Prof. Pap., 1350*, 641-689, 1987.

Walker, D., Behavior of mass absorption coefficients near absorption edges: Reynolds' method revisited, *Am. Mineral., 58*, 1,069-1,072, 1973.

West, H. B., D. C. Gerlach, W. P. Leeman, and M. O. Garcia, Isotopic constraints on the origin of Hawaiian lavas from the Maui Volcanic Complex, Hawaii, *Nature, 330*, 216-220, 1987.

Wright, T. L., Chemistry of Kilauea and Mauna Loa lavas in space and time, *U.S. Geol. Surv. Prof. Pap., 735*, 1-49, 1971.

Wright, T. L., and R. S. Fiske, Origin of the differentiated and hybrid lavas of Kilauea volcano, Hawaii, *J. Petrol. 12*, 1-65, 1971.

Yang, H.-J., and F. A. Frey, Submarine lavas from Mauna Kea volcano, Hawaii: Implications for Hawaiian shield processes, *J. Geophys. Res., 99*, 15,577-15,594, 1994.

Yang, H.-J., F. A. Frey, J. M. Rhodes and M. O. Garcia, Evolution of the Mauna Kea volcano: Inferences from lava compositions recovered in the Hawaii Scientific Drilling Project, *J. Geophys. Res.*, this issue.

J. M. Rhodes, Department of Geosciences, University of Massachusetts, Morrill Science Center, Box 35820, Amherst, MA 01003. (e-mail: jmrhodes@eclogite.geo.umass.edu)

(Received May 3, 1995; revised November 21, 1995; accepted November 29, 1995.)